We are IntechOpen,
the world's leading publisher of
Open Access books
Built by scientists, for scientists

6,900
Open access books available

185,000
International authors and editors

200M
Downloads

154
Countries delivered to

Our authors are among the

TOP 1%
most cited scientists

12.2%
Contributors from top 500 universities

CLARIVATE ANALYTICS
BOOK CITATION INDEX
INDEXED

WEB OF SCIENCE™

Selection of our books indexed in the Book Citation Index
in Web of Science™ Core Collection (BKCI)

Interested in publishing with us?
Contact book.department@intechopen.com

Numbers displayed above are based on latest data collected.
For more information visit www.intechopen.com

Characterization and Evaluation of Surface Modified Titanium Alloy by Long Pulse Nd:YAG Laser for Orthopaedic Applications: An *Invivo* Study

M. E. Khosroshahi

Laser and Nanobiophotonics Lab., Biomaterial Group, Faculty of Biomedical Eng.,
Amirkabir University of Technology, Tehran,
Iran

1. Introduction

The overall reaction of the living system body to a foreign material implant is governed by a number of factors that determine whether the implant is accepted or rejected. Biocompatibility and biosafety are considered to imply that the clinical application of a biomaterial should neither cause any adverse reaction nor endanger the life of a patient. Generally, parameters determining the biocompatibility are: i- tissue as a host and ii-implant as a guest. Animal testing is an inherent component of biocompatibility testing. The use of in vitro methods can reduce the extend of animal testing and significantly reduce time and cost of testing. Knowledge of basic mechanisms of cell–material interaction and better understanding of ongoing processes at the cellular level during interaction of anchorage dependent cells can aid in the development of new biomaterials.

Factors affecting the tissue–implant interface from biocompatibility point of view include: general health, immunity factors, roughness, surface porosity, chemical reactions, corrosion and cytotoxicity. Thus, the surface characterization of biomaterials is particularly important if the biocompatibility of implants is to be understood. Possible mechanisms through which a biomaterial can interact with a metallic implant is illustrated in Fig. 1.

A variety of surface properties are believed to be responsible for the favorable performance of titanium implants, in particular the presence of a chemically very stable oxide film protecting the underlying metal from corrosion, the moderate charge of he surface under biological conditions, the very low concentration of charged species within the dissolution products and a dielectric constant ε for titanium oxide close to that of water (ε =78). The result is that the titanium surface does not lead to excessively strong interaction (and denaturation) with proteins in the extra cellular matrix; rather the surface is in some way water like, interacting gently with the hydrophilic outer surface of the protein molecules. Nature of interaction between osteoblast cells and their substrate can influence the ability of these cells to produce an osteoid matrix around an implant which in turn will determine the fate of the implant. Attachment of anchorage dependent cells is the first step in the process of cell surface interactions which in turn can affect subsequent cellular and tissue responses.

Cells attach to substrates through contact sites which are classified as focal contacts. It is important to understand the nature of contact of cells interacting with biomaterials. Changes in cell morphology can be studied using different microscopic techniques like phase contrast and electron microscopy. In case of implants intended for orthopaedic application where close apposition with bone cells is required for better osteointegration, cell attachment and adhesivity play an important role.

2.1 Kinetics of cell - bioimplants interaction
Protein adsorption

Titanium implants were first introduced by Branemark in the early 1970s [Branemark et al., 1977] and have been widely used in the medical and dental fields with excellent clinical results. In addition, bone appears to bond with the titanium oxide layer following implantation, a phenomenon termed osseointergation. However, little is known about the specificity of this process and still less is known about the proteins that adsorb on the titania surfaces. In terms of the host tissue- biomaterial interaction the role of adsorbed proteins is likely to be an important one because subsequent events may depend on the composition and conformation of this protein layer and its tendency to change over time. The final protein film may trigger the activation of complementary are coagulation cascades and other inflammatory response [Kazatchkine & Carreno, 1988; Ziats et al., 1988].

Macromolecules adsorption is a complicated process but for simplicity it can be summarized as follow:

1. The encounter of soluble molecules with surface which is determined by diffusion constants of concentration of different species.
2. A reversible binding of molecules to surface which means that bound molecules may be detached in a very short time.
3. Constant modification of the composition of adsorbed layers ie. some species may be replaced by more adhesive ones. This is the basis of Vroman effect.
4. Progressive conformation changes of adsorbed proteins hence strengthening adhesion.
5. Possibility of continues adsorption with formation of multiple protein layers.

As it is seen in Fig. 1 there are various forces such as Vander walls, bipolar, hydrogen, ionic and covalent that can play an important role in adsorption of protein molecules.

The kinetics of adsorption of proteins to solid surfaces generally consist of a very rapid initial phase that is diffusion limited, followed by a slower phase upon approach to the steady-state value. In the initial phase, the proteins typically adsorb a quickly as they arrive at the relatively empty surface. In the later, slower phase, it is presumably more difficult for the arriving proteins to find and fit into an empty spot on the surface. In as short a time as can be measured after implantation in a living system (<l sec), proteins are already observed on biomaterial surfaces. In seconds to minutes, a monolayer of protein adsorbs to most surfaces. The protein adsorption event occurs well before cells arrive at the surface. Therefore, cells see primarily a protein layer, rather than the actual surface of the biomaterial.

It is thought that the particular properties of surfaces, as well as the specific properties of individual proteins, together determine the organization of the adsorbed protein layer, and that the nature of this layer in turn determines the cellular response to the adsorbed surfaces. The soluble proteins differ from the insoluble proteins is many ways, including the

fact that they are less regular in their amino acid composition and three dimensional structure. The soluble proteins are therefore difficult to describe, this diversity originates in the linear sequence of amino acid that uniquely characterizes each protein.
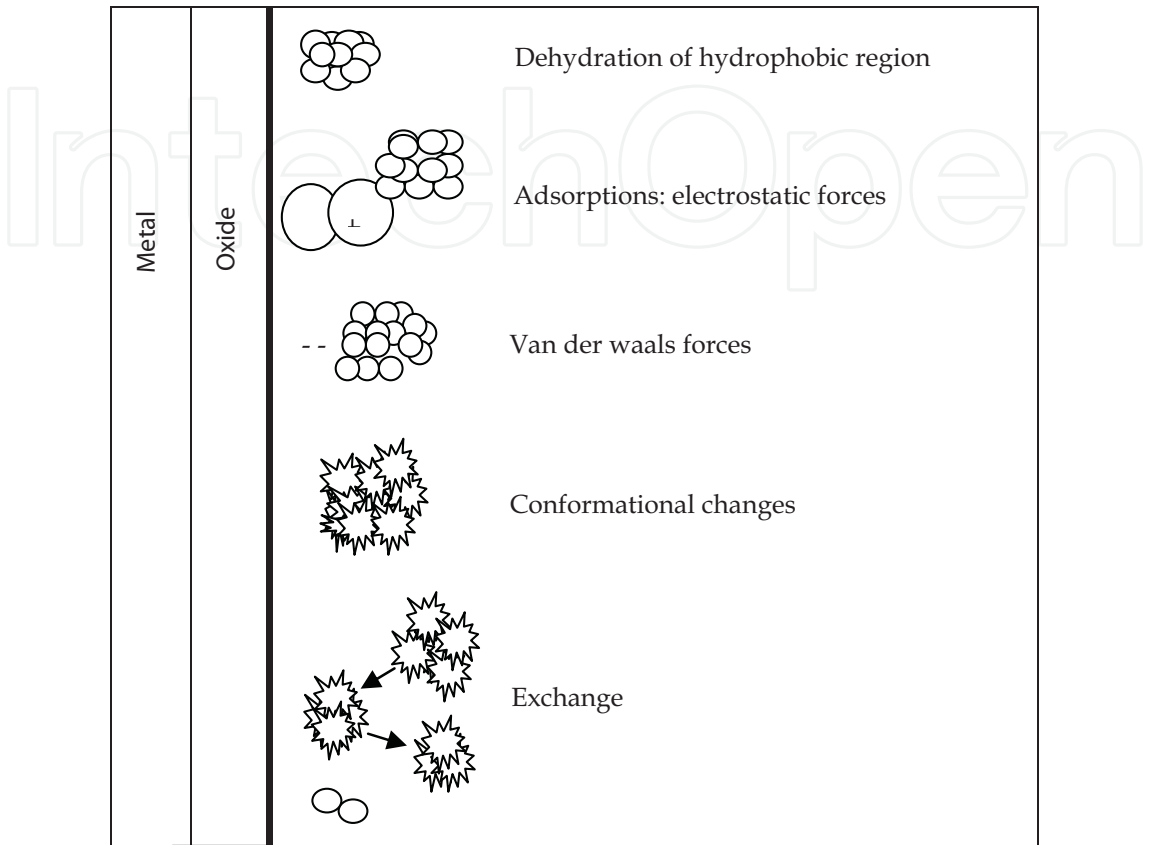

Fig. 1. Routes of protein adsorption to implant surface

It is important to note the particular structure assumed by a protein which in fact is a unique arrangement of the amino acid sequence in three – dimensional space exists for each protein. Furthermore, the spatial arrangement results in the hydrophobic residues preferentially located "inside" the protein where they are shielded from water, while the ionized and polar residues are usually on the outside of the proteins and in contact with the aqueous phase.

This spatial arrangement of the amino acids in proteins has a direct bearing on the interaction of proteins with surfaces because it means that the many residues "buried" inside the proteins may not be able to participate in bond formation with the surface. The folded proteins structures have densities of about 1.4 g/cm^3 in comparison with water's density of 1.0, or the density of most synthetic polymers of about 1.1, this basic fact about proteins reflects their tightly folded structure. Therefore, depending on the two major driving forces for adsorption, namely, the relative bulk concentration of each protein and its intrinsic surface activity, the outcome of the competitive process of adsorption is an adsorbed layer that is richer in some proteins than others; the surface composition differ from the bulk composition.

The thermodynamics of protein adsorption are not easily characterized because the process appears to be essentially irreversible. Because adsorption is irreversible, the calculation of an

equilibrium binding constant from a plot of adsorption versus bulk concentration, and its conversion to a free energy value in the usual way, is not a valid method to obtain thermodynamic information. The enthalpy of the adsorption process has been observed to vary a great deal. The observation of positive enthalpies upon spontaneous adsorption to certain surface must mean that the process is entropically driven in these cases. The net negative free energy characteristic of a spontaneous process means that $T\Delta S$ is greater than the positive ΔH term in the formula $\Delta G=\Delta H-T\Delta S$. More generally, all protein adsorption processes are thought to be strongly driven by entropic changes. The important of entropic factors in this process can easily be envisaged to arise from changes in water binding to the surface and the protein as well as limited unfolding of the protein on the surface.

The orientation of proteins in the adsorbed phase must also be considered because the proteins are not uniform in properties or structure across their surface. As far as is known, proteins are not very free to rotate once adsorbed, owing to multiple bonding is exposed to the bulk phase. The reactions of proteins in the adsorbed phase may be broadly classed into noncovalent reactions represented by structural transitions, and covalent reactions, such as those that occur with proteins complements.

Cell – adhesion

There is no need to emphasize the potential interest of controlling or even predicting the outcome of encounters between cells and artificial surfaces. Indeed, such knowledge would greatly facilitate the production and use of biomaterial. Three sequential steps of cell surface interaction are considered as:1-protein adsorption , 2-formation of adhesive ligand–receptor bonds, 3-triggering specific cell function such as apoptosis, proliferation, migration (locomotion), differentiation or activation. Cell adhesion is a well – studied mechanism of cell communication. Adhesion is a form of mechanical linkage, of cells to cells and cells to the ECM, and is critically involved in cellular signaling events that control proliferation, survival, apoptosis, shape, polarity, motility, and differentiation. Adhesion is mediated by transmembrane proteins, which connect the interior of the cell to its extra cellular environment (Fig. 2). One major feature biological adhesion that is different from non-biological adhesion such as with household and industrial adhesives is that the former is mediated by chemical signals that often positively or negatively feedback to adhesion and subsequent cell behaviour. In other words, cell adhesion is more than a simple glue to hold cells and tissues together; it is also a critical signaling platform. Integrins and cadherins are two principal classes of molecules mediating primarily cell-ECM and cell-cell adhesion respectively.

Integrins are the best–understood class of adhesion receptors [Hynes, 2002]. They mediate both cell -ECM and cell-cell adhesion, differing based on the cell type and the type of receptor used in the interaction. Integrins, composed of α-β subunit heterodimer, assemble into 24 distinct integrins and bind to proteins in the ECM such as fibronectin, collagen and laminin [Hynes, 2002]. The binding of integrins initiates clustering of integrins to form structures and the recruitment of a host of signaling and adaptor proteins as well as the actin cytoskeleton [Geiger & Bershadsky, 2001]. These focal adhesions are involved in the signaling events that lead to proliferation, motility, cytoskeletal organization, and cell survival [Geiger & Bershadsky, 2001].

Cadherins mediate adhesive contact between cells in structures called adherens junctions, and play a vital role in morphogenec events during development. The best studied of these

are the classical cadherins, which mediate adhesion between adjacent cells by forming homotypic junctions at sites called adherens junctions, and are linked intracellularly to the actin cytoskeleton through beta-catenin and alpha-actinin. Similar to integrins, cadherins too have a mechanical and signaling role. Along with the mechanical that adhesion plays in tissue cohesion, cadherins, like integrins, transmit specific signals to the cell interior through proteins at the adhesion site [Shay-Salit et al., 2002; Yap & Kovacs, 2003]. Both integrin and cadherin adhesions are biochemically regulated and are both dynamic and reversible. Normal cell processes such as the rounding of spread cells during mitosis, cell sorting and migration during embryogenesis, or disease processes such as cancer cell metastasis involve active changes in adhesion strength between cell-ECM and cell-cell contacts. Also, adhesive signals regulate many of the same cell function that soluble growth factors do. Adhesion and growth factor pathways are cooperative: for example, anchorage dependent cells do not grow in the absence of adhesion when they are placed in suspension even in the presence of saturating amounts of growth factors, neither do they grow in the absence of growth factors even when adherent. It is only when both adhesive and growth factor signals are present that growth pathways are optimally activated in cells [Zhu & Assoian, 1995].
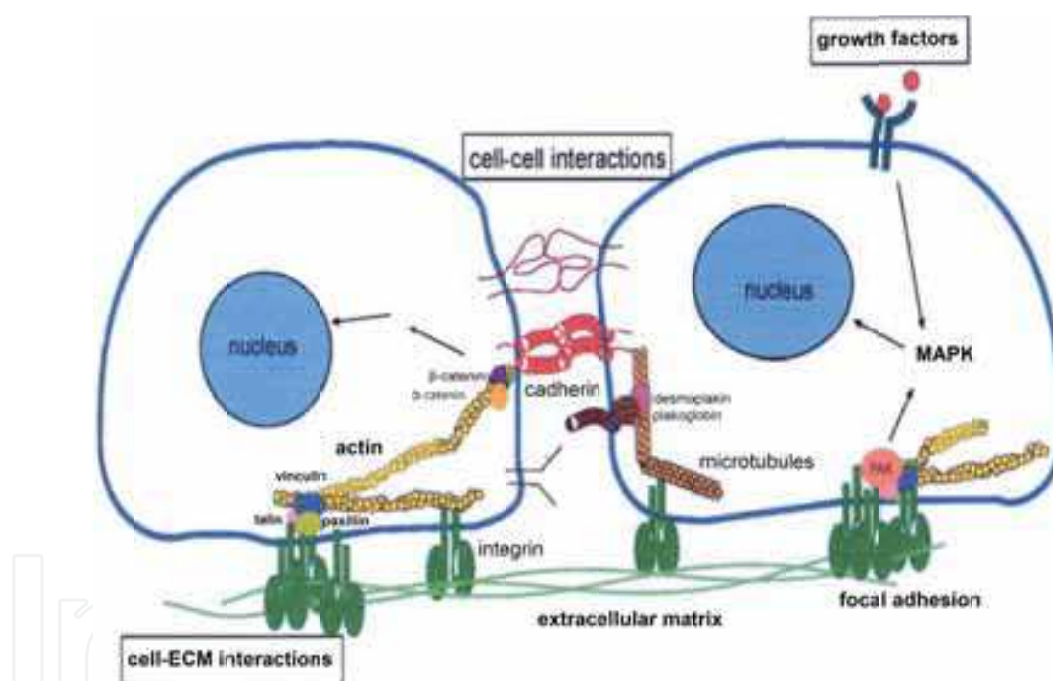

Fig. 2. Representation of the cell–biomaterial surface interaction

However, the effects observed for a given protein have been found to vary substantially depending on the nature of the underlying substrate and the method of immobilization [Neff et al., 1999; Juliano, et al., 1993]. Because cells interact with ECM proteins through receptors that bind to localized regions within their proteins ligands, the biological activity of proteins on the surface will depend upon whether specific active peptide sequence in specific proteins are accessible to the arriving cells [Yamada, 1991]. Many of the ECM proteins, like fibronectin, laminin vitronectin, von Willebrand factor, carry a sequence of amino acid, arginine-glycin- aspartic acid (RGD) to which cells can bind using specific surface receptors called integrins [Pierschbacher & Ruoslahi, 1984; Ruoslahi &

Pierschbacher, 1987]. Integrin-mediated binding of cells is the foundation for cell growth and differentiation and is the dominant mechanism by which cells communicated with noncellular surroundings [Ruoslahi, 1991].

In brief, cell adhesion is involved in various natural phenomena such as embryogenesis, maintenance of tissue structure, wound healing, immune response, metastasis as well as tissue integration of biomaterial. Surface characteristics of materials, whether their topography, chemistry of surface energy, play an essential part in osteoblast adhesion on biomaterials. Thus attachment, adhesion and spreading belong to the first phase of cell/material interactions and the quality of this first phase will influence the cells' capacity to proliferate and to differentiate itself on contact with the implant.

Cell spreading is a combined process of continuing adhesion and cytoplasm contractile meshwork activity. Cell adhesion and spreading are influenced by the physicochemical characteristics of the underlaying solid surface. Other important parameters involved in cell-adhesion are: 1- surface charge, 2- topography, 3- porosity, 4- grooves, 5- mechanicl forces, 6- texture and 7- cellular locomotion. The high ionic strength of the physiological environment and the rapid establishment of ionic equilibrium indicate that surface electrical properties do not significantly influence the formation of initially adsorbing protein layers or adhering cells. The surface topograghy of a biomaterial can be classified according to roughness, texture, and porosity. Porosity is used on a large scale to promote anchorage of biomaterials to surrounding tissue. Grooved substrata were found to induce a certain amount of cellular orientation and locomotion in the direction of the grooves. Applying grooved substrata will therefore induce cell contact guidance. Mechanical forces around an implant, especially in combination with a rough surface, induce abundant formation of fibrous tissue, owing to the constant irritation of the cells. The texture of an implant surface and its morphology can be adapted to the clinical purpose of the biomaterial by such approaches as changing the fabrication process (e.g., woven, knitted, fibrous, grooved, veloured, smooth). Cellular locomotion can be directed by various gradients in the cell environment. For example, after implantation of a biomaterial, granulocytes are attracted by a negative oxygen gradient. Fibroblasts are attracted by agents produced by macrophages.

Orthopaedic implants

Titanium and titanium alloys are largely used as implant materials because of their high in vitro and in vivo biocompatibility and load bearing. It is well established that oseteointegration is an important property of titanium implant surfaces and that the current success rate is satisfactory [Feng et al., 2003; Puleo et al., 1989; Albrektsson et al., 1981]. Osseointegration is a term introduced by Beraceras et al., 1977 to describe a loaded, stable implant in direct contact with bone. Osseointegrated implants differ from ingrown ones that are dependent upon bone growth into surface macroscopic features or irregularities. By contrast, osseointegration is dependent on tissue ingrowth into minute surface features, such as the fundamental asperities of a smooth surface or as postulated for surfaces of various crystalline calcium phosphates (such as calcium hydroxyapatite) or amorphous, bioactive glasses, on direct chemical bonding between tissue and implant. Nevertheless, some concern remains as to the effects of vanadium and aluminum which are known to be cytotoxic [Khosroshahi[a] et al., 2007; Deppe et al., 2005]. The chronology of the metal alloys is shown in table 1.

Characterization and Evaluation of Surface Modified Titanium Alloy
by Long Pulse Nd:YAG Laser for Orthopaedic Applications: An *Invivo* Study
175

Alloy	Year	Application	Performance issues
Vanadium steel	1912	Bone plates	Corrosion problems
Cast Co-Cr-Mo	1937	Dental devices	Well accepted
Cast Co-Cr-Mo	1938	Orthopaedic implants	Well tolerated, adequate strength
302 stainless steel	1938	Bone plates /screws	corrosions resistance
316 stainless steel	1946	Trauma implants	Better corrosions resistance and strength
Titanium	1965	Hip implants (England)	Corrosion resistance, tissue acceptance
316LVM stainless steel	1968	Trauma implants	Further improvements in corrosion
MP35N	1972	European hip prostheses	High strength
Ti-6Al-4V	1974	Trauma implants	High strength, biocompatibility
Ti-6Al-4V	1976	Hip prostheses	High strength, low modulus
Forged Co-Cr-Mo	1978	Hip prostheses	Highest fatigue strength
22-13-5 stainless steel	1981	Hip implants, trauma	High strength, forgeability
Ti-6A1-7Nb	1982	Hip implants	High strength, biocompatibility
Cold-forged 316LVM	1983	Compression hip screw	High strength
Zirconium 2.5 Nb (zirconia cated)	1994	Joint prostheses	Improved wear resistance, Biocompatibility

Table 1. Chronology of metal alloys in orthopaedic applications

Bone – cell adhesion

The attachment phase occurs rapidly and involves short-tem events like physicochemical linkages between cells and materials involving ionic forces Van der Waal forces, etc and the adhesion phase occurs in the longer term and involving various biological molecules: extra cellular matrix proteins, cell membrane proteins, and cytoskeleton proteins which interact together to induce signal transduction, promoting the action of transcription factors and consequently regulating gene expression. Proteins involved in osteoblast cells adhesion are: 1-Extra cellular matrix proteins, 2- Cytoskeleton proteins, 3- Adhesion molecules.

1.2 Surface modification of Ti-6Al-4V alloy by long Nd:YAG laser for orthopaedic applications

It is possible to change localized areas of metals in order to obtain both compositions and microstructures with improved properties. Titanium and titanium alloys are the most frequently used material for load-bearing orthopaedic implants, due to their specific properties such as high corrosion resistance, surface oxidation layer, high strength and high-temperature resistance [Feng et al., 2003; Ducheyne & El-Ghannam, 1994; Kelly et al., 2003; Wang et al., 2003; Hsu et al., 2004; Tian et al., 2005]. Titanium and its alloys' application like

any other biomaterials involve the creation of at least one interface between the material and biological tissues. Biocompatibility and bioactivity of biomaterials rely on the interactions that take place between the interface of the biomaterials and the biological system [Wang & Zheng, 2009]. It is generally believed that proteins adsorbed on implant surface can play an important role in cell-surface response. Different proteins such as collagen, fibronectin and vitronectin which are acting as ligands are particularly important in osteoblast interaction with surface. Ligands are the junctions which facilitate adhesion of bone cells to implant surface. In another word, more ligand formation implies a better cell-surface interaction [Tirrell et al., 2002; Anselme et al., 2000]. *In vitro* studies can be used to study the influence of surface properties on processes such as cell attachment, cell proliferation and cell differentiation. However, *in vivo* studies must be performed to achieve a complete understanding of the healing process around implants. Previous studies have shown that surface characteristics named above have a significant influence on adhesion, morphology and maturation of cultured osteoblasts [Davies, 1996; Thomas et al., 1997; Cooper et al., 1998; Masuda et al., 1998]. Also, it has been demonstrated that for primary bovine osteoblasts, the wettability is one of the key factors [Meyer, 1993]. In our studies [Khosroshahi[a] et al., 2007; Khosroshahi[b], 2007; Khosroshahi[a] et al., 2008; Khosroshahi[b] et al., 2008; Khosroshahi et al., 2009] it is shown that the wettability of the surface can provide a better spreading condition for osteoblast cells due to reduced contact angle. Bearing in mind that the adhesion of bone cells to implant surface consists of two stages. In primary stage the cells must get close enough to surface in an appropriate distance known as focal distance over which the cells can easily be spread over it. In this respect, the wettability can be effective in providing a preferred accessability to surface and thus reaching the focal distance. The secondary stage includes cell-cell attachment which obeys the regular biological facts.

Interface reactions between metallic implants and the surrounding tissues play a crucial role in the success of osseointegration. The titanium and its alloys like some other medical grade metals are the materials of choice for long-term implants. The effect of implant surface characteristics on bone reactions has thus attracted much attention and is still considered to be an important issue [Albrektsson & Johansson, 2001; Buchter et al., 2005; Buchter et al., 2006]. So far as the surface characteristics of the implants are concerned, two main features that can influence the establishment of the osseointegration are the physico-chemical properties and the surface morphology. Cell adhesion is involved in various phenomena such as embryogenesis, wound healing, immune response and metastasis as well as tissue integration of biomaterial. Thus, attachment, adhesion and spreading will depend on the cell-material interaction and the cell's capacity to proliferate and to differentiate itself on contact with the implant [Chung et al., 2003; Bigerelle & Anselme, 2005].

Cell behaviour, such as adhesion, morphologic change and functional alteration are greatly influenced by surface properties including texture, roughness, hydrophilicity and morphology. In extensive investigations of tissue response to implant surfaces, it has been shown that surface treatment of implant materials significantly influences the attachment of cells [Cheroudi et al., 1995; Curtis & Wilkinson, 1998; Brunette & Cheroudi, 1999 ; Lavose-Valereto et al., 2001; Curtis & Clark, 2001 ; Sowden & Schmitz, 2002; Heinrich et al., 2008]. Additionally, these modified surfaces must resist both the mechanical wear and the corrosion [Sighvi & Wang, 1998]. It is therefore important to evaluate systematically the role of different surface properties and to assess the biological performance of different implant materials.

Titanium as a biomaterial implant has an excellent biocompatibility due to the fact that it is highly inert and is not soluble in body fluids and forms a protective oxide layer on the surface [Burser & Schenk, 1991; Breme & Helsen, 1998]. However, pure titanium could leave metal debris in the tissue due to the higher tendency to produce wear in fretting conditions. Therefore numerous titanium alloys like Ti6Al4V with improved physical and mechanical properties have been developed.

The surface morphology, as well as manipulation with the physical state and chemical composition of implant surface may be significant for bone-implant integration. Surfaces are treated to facilitate an intimate contact between bone and implant. So, the tissue response to an implant involves physical factors, depending on implant design, surface topography, surface charge density, surface free energy and chemical factors associated with the composition of the materials. These substrate characteristics may directly influence cell adhesion, spreading and signaling, events that regulate a wide variety of biological functions [Sikavitsas et al., 2001; Sun et al., 2001; Ronold & Ellingsen[a], 2002; Ronold & Ellingsen[b], 2002; Ronold et al., 2003]. Numerous surface treatments including Ion implantation [Beraceras et al., 2002, Tan et al., 2003; Assmann et al., 2007], coating [Vercaigne et al., 1998; Ong et al., 1997; Toth et al., 2002; Morra et al., 2003; Tian et al., 2004; Eisenbarth et al., 2007], shot blast [Darvell et al., 1995; Kawaura et al., 2002; Aparicio et al., 2003], machining [Sahin & Sur, 2004], plasma spray [Khor et al., 1999; Yang & Change, 2001], plasma nitrid [Galvanetto et al., 2002], nitrogen diffusion hardening [Venugopalan et al., 2000] are some of the relatively older techniques in the field of material processing which can be used to change implant's surface topography. But perhaps the laser-assisted method has recently received more attention and has been successful in meeting the new objectives in this field which is mainly because of its wavelength selectivity, coherency, very low thermal or mechanical damage, high accuracy, control and less pollution during laser treatment process.

In fact, optical and kinetics of laser parameters like fluence and pulse number as well as surface physical parameters will affect this process [Gaggl et al., 2000; Wang et al., 2000; Fancsaly et al., 2002; Hollander et al., 2005; Hao[a] et al., 2005]. For example, surface modification of metals by CO_2 [Tritca et al., 2001; Ghoo et al., 2001], HF [Deka et al., 1980; Khosroshahi, 2004], Nd:YAG [Peyer et al., 2000; Yang et al., 2004; Trtica et al., 2009], and diode lasers [Slocombe et al., 2000; Majumdar et al., 2005], titanium alloy by Nd:glass [Joob-Fancsaly et al., 2002], KrF [Deppe et al., 2005], XeCl [Tritca et al., 2005], diode lasers [Hao[b] et al., 2005] and However the recent studies on this subject using short Nd:YAG laser pulses have been performed as *In vitro* with some limited but informative results [Arisu et al., 2006; Turner et al., 2007; Mirhosseini et al., 2007]. Also recently a femtosecond laser was used for surface treatment of titanium in order to determine the potentiall of this technology for surface structuring of titanium implants [Vorobyev & Guo, 2007]. Thus, the success of uncemented orthopaedic implants depends largely upon the body's ability to synthesize new bone directly onto the surface of the device. This gap allows micromotion of the implant, which loosense the device and ultimately leads to implant failure. Some researchers have attempted to circumvent capsule formation by coating metal implants with the synthetic bone analogue, hydroxyapatite (HA). The synthesis and deposition of new bone onto an implant requires the attachment of osteoblast precursor cells to the implant surface, as well as the subsequent differentiation of these cells. Both of these processes are likely mediated by the integrin family of cell adhesion receptors. Thus, the main intension of this work is to extend the earlier research by carrying out some detailed *In vitro* and *In vivo*

experiments using a long pulse (200μs) Nd:YAG laser radiation on surface physico-chemical changes, surface wettability, corrosion resistance, microhardness and direct osteoblast cells adhesivity of Ti6Al4V with respect to possible orthopaedic applications. Finally, to assess and compare the effects of physico- chemical modifications made on laser treated surface (LTS).

2. Materials and methods

Sample preparation

Rectangular–shaped specimens with 20×10 mm dimensions and the thickness of 2 mm, were made from a medical grade Ti6Al4V (ASTM F136, Friadent, Mannheim- Germany- GmbH) with chemical formulation Ti(91.63%) Al(5.12%) V(3.25%). The samples were divided into three groups of untreated (7 samples), laser treated (14 samples). Prior to treatment, all samples were cleaned with 97% ethanol and subsequently been washed twice by distilled water in an ultrasonic bath (Mattachanna, Barcelona-Spain). A final rinse was done by de-ionized water at a neutral pH to ensure a clean surface is obtained. Finally, an optical microscope with magnification of x20 was used to ensure that no particles were left on the sample surface.

Experimental setup

Surface treatment was performed by Nd: YAG laser with 1.06μm wavelength, 200μs pulse duration and pulse energy of 50 J. The output beam was suitably imaged on to the target surface in a 500 μm spot diameter where it scanned the surface at a constant velocity using a motorized XYZ translator. All the experiments were carried out in air at pulse repetition frequency of 1Hz. In order to achieve the optimum surface treatment conditions, the melting, evaporation thresholds and variation of etch depth with fluence were evaluated. Etch depth per pulse variation as a function of laser fluence can be calculated from equation (1).

$$X = \alpha^{-1} \ln\left(F/F_t\right) \tag{1}$$

Where, X is the etch depth, α is absorption coefficient and F_t is the threshold fluence. The samples were then sterilized by de-ionized water.

Surface roughness

The surface micro roughness (R_a) measurements were carried out using a non-contact laser profilemeter (NCLP) (Messtechnik, Germany) equipped with a micro focus sensor based on an auto focusing system. R_a is the arithmetical mean of the absolute values of the profile deviations from the mean line. Five two-dimensional NCLP profiles were obtained for each surface over a distance of 3.094 mm with a lateral resolution of 1μm using a Gaussian filter and an attenuation factor of 60% at a cut-off wavelength of 0.59 mm . The roughness parameters were calculated with the NCLP software similar to that described by Wieland et al. [Wieland et al., 2001].

Surface hardness

Surface microhardness test was carried out with 50 gram load in 10 seconds by a diamond squared pyramid tip (Celemx CMT, Automatic). Each related test was considered at 5 points and reported as an average. The Vickers diamond pyramid hardness number is the applied load divided by the surface area of the indentation (mm²) which could be calculated from below equation:

$$VHN = \left\{2FSin(136°/2)\right\}/d^2 \qquad (2)$$

This equation could be re-written approximately as:

$$VHN = 1.854\left(F/d^2\right) \qquad (3)$$

Where F is load in Newton, d (mm) is the arithmetic mean of the two diagonals, d_1 and d_2 in mm and VHN is Vickers hardness. The Vickers diamond pyramid indenter is grounded in the form of a squared pyramid with an angle of 136° between faces. The depth of indentation is about 1/7 of the diagonal length. When calculating the Vickers hardness number, both diagonals of the indentation are measured and the mean of these values is used in the above formula with the load used to determine the value of VHN.

Corrosion tests

The standard Tafel photodynamic polarization tests (EG&G, PARC 273) were carried out to study the corrosion behaviour of specimens in Hank's salt balanced physiological solution at 37ºC. The procedure for preparing the Hanks solution is schematically shown in The metal corrosion behaviour was studied by measuring the current and plotting the E-logI (Voltage – Current) diagram. The corrosion rate (milli per year (mpy)) was determined using equation:

$$C.R. = 0.129\left(M/n\right)\left(I_{corr}/\rho\right) \qquad (4)$$

Where M is the molecular weight, n is the charge, I_{corr} is the corrosion current and ρ is the density.

Surface tension

The surface energy of the samples were determined by measuring the contact angle (θ) of test liquids (diiodo-Methane and water; Busscher) on the titanium plates using Kruss-G40-instrument (Germany).The geometric mean equation divides the surface energy in to two components of dispersive and polar and when combined with Young's equation it yields:

$$\gamma_{1v}\left(1+\cos\theta\right) = 2\left(\gamma_1^d \cdot \gamma_s^d\right)^{0.5} + 2\left(\gamma_1^p \cdot \gamma_s^p\right)^{0.5} \qquad (5)$$

Equation (5) can be rearranged as by Ownes-Wendt-Kaeble's equation:

$$\gamma_{1v}\left(1+\cos\theta\right)/\left(\gamma_1^d\right)^{0.5} = \left(\gamma_s^p\right)^{0.5}\left[\left(\gamma_1^p\right)^{0.5}/\left(\gamma_1^d\right)^{0.5}\right] + \left(\gamma_s^d\right)^{0.5} \qquad (6)$$

Where s and l represent solid and liquid surfaces respectively, γ^d stands for the dispersion component of the total surface energy (γ) and γ^p is the polar component.

2.1 In vivo test
Anesthetization

Before depilation of the operation site, the animal was completely anesthetized with midazolam (Dormicum®, Roche, Switzerland) 2.5 mg/Kg intravenously (IV). With any sign of recovery during operation, diluted fluanisone/fentanyl (Hypnorm®, India) was injected slowly until adequate effect was achieved, usually 0.2 ml at a time.

Animal implantation

One untreated sample and two LTS were implanted on femur bone of an eight months male goat weighing 30 Kg. Specimens were steam sterilized before implantation in an autoclave (Mattachnna, Barcelona-Spain). The steam sterilization was conducted under 132 °C, 2 bar and in 45 minutes. All the specimens were labeled by separate codes for further studies. The operation site was shaved and depilated with soft soap and ethanol before surgery; the site was also disinfected with 70% ethanol and was covered with a sterile blanket. In order to proceed with implantation, cortex bone was scraped by osteotom (Mattachnna, Barcelona-Spain) after cutting the limb from one-third end in lateral side and elevating it by a self – retaining retractor. Copious physiological saline solution irrigation was used during the implantation to prevent from overheating. To ensure a stable passive fixation of implants during the healing period, they were stabilized by size 4 and 8 titanium wires (Atila ortoped®, Tehran-Iran) without any external compression forces (Fig. 3).

Fig. 3. Placement of implants in the femur bone of the goat
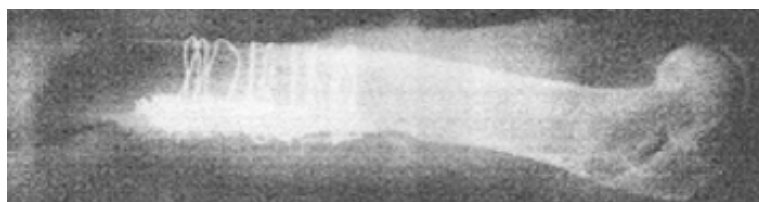
Fig. 4. The X-ray of implants wired to the bone

| (a) | (b) |

Fig. 5. Implant removal from the femur bone of the goat: (a) before detachment of the wires, (b) the foot-print of the implants on the bone

After the operation the animal was protected from infection by proper prescribed uptake of Penicillin for first four days and Gentamicine for second four days. During the eight days of

Characterization and Evaluation of Surface Modified Titanium Alloy
by Long Pulse Nd:YAG Laser for Orthopaedic Applications: An *Invivo* Study
181

recovery, the goat was administrated with multi-vitamins to help to regain its strength. During this period, the goat was kept in an isolated space under room temperature, ordinary humidity, lightening and air condition, and before it returns to its natural life environment, X-ray radiographs (Fig. 4) were taken in order to ensure that the implant has not been displaced during the maintenance period. It was observed that calus bone had grown in the vicinity of the implant. After five months the animal was sacrificed and the specimens were removed (Fig. 5).

The experiments had been approved by the Yazd School of Veterinary Science (Iran) and its animal research authority and conducted in accordance with the Animal Welfare Act of December 20th 1974 and the Regulation on Animal Experimentation of January 15th 1996. The explantation procedure was performed by first cutting the upper and lower section of femur bone using an electric saw and then the implant together with its surrounding tissues was placed in 4% formalin solution for pathological assessment and SEM.

Cell analysis

Osteoblast cells spreading (ie.lateral growth) on the six implants (three samples for imaging and three samples for coulter counter) was analyzed after removal by SEM(stero scan 360-cambridge) and their spreading condition in a specific area was studied using Image J Program software in three separate regions of each specimen at frequency of 10 cells per each region. The number of attached cells in 1 cm² area of each specimen was calculated by a coulter counter (Eppendorf, Germany) using enzyme detachment method and Trypsin-EDTA (0.025 V/V) in PBS media at pH = 7.5. The final amount of attached cell can be studied by plotting cell detachment rate versus time.

Histopathology

Surrounding tissues of specimens were retrieved and prepared for histological evaluation. They were fixed in 4% formalin solution (pH = 7.3), dehydrated in a graded series of ethanol (10%, 30%, 50%, 70% and 90%) and embedded in paraffin after decalcification. Then, 10 µm thick slices were prepared per specimen using sawing microtome technique. A qualitative evaluation of macrophage, osteoblast, osteoclast, PMN, giant cells, fibroblast, lymphocyte was carried out by Hematoxylin and Eosin stain and light microscopy (Zeiss, Gottingen-Germany). The light microscopy assessment consisted of a complete morphological description of the tissue response to the implants with different surface topography. Osteoblasts can be in two states; (a) active, forming bone matrix; (b) resting or bone-maintaining. Those make collagen, glycoproteins and proteoglycans of bone the matrix and control the deposition of mineral crystals on the fibrils. Osteoblast becomes an osteocyte by forming a matrix around itself and is buried. Lacunae empty of osteocytes indicate dead bone. Osteoclast, a large and multinucleated cell, with a pale acidophilic cytoplasm lies on the surface of bone, often an eaten-out hollow-Howship,s lacuna. Macrophages, are irregularly shaped cells that participate in phagocytosis.

SEM of adhered cells

After implants removal, all three group implants were rinsed twice with phosphate buffer saline (PBS) and then fixed with 2.5% glutaraldehyde for 60 minutes. After a final rinse with PBS, a contrast treatment in 1% osmium tetroxide (merck) was performed for 1 hour, followed by an extensive rinsing in PBS and dehydration through a graded series of ethanol from 30% to 90% as described in histology section. After free air drying, surfaces were thinly sputter coated with gold (CSD 050, with 40 mA about 7 min). Cell growth on implanted specimens and their spreading condition in a specific area was analyzed using Image J Program software in three separate regions of each specimen for 10 cells per each region.

Statistical analysis

All calculated data were analyzed by using a software program SPSS (SPSS Inc., version 9.0). The results of variance analysis were used to identify the differences between the cells spread area of the treated and cleaned un-treated samples ($p \leq 0.05$).

3. Results

3.1 Characterization of surface topography

Optical and Mechanical Effects

Fig. 6 indicates the variation of etch depth per pulse with the laser fluence where the metal absorption coefficient (α) can be determined from the slope of the curve using the well known beer logarithmic equation (Eq.1). From Equation 66 the values of α and F_t were found $5 \times 10^3 cm^{-1}$ and 73 Jcm^{-2}, respectively. It is interesting to notice that, in our case, the interaction of laser radiation with metal surface can be divided into four different regions:
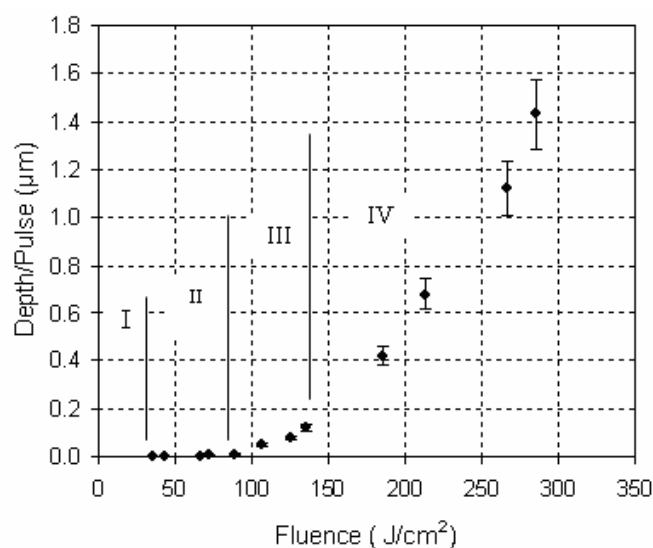
Fig. 6. Variation of etch depth as a function of fluence

In zone I (0-30 Jcm^{-2}) no morphological changes was observed but beyond that where zone II (30-70 Jcm^{-2}) commences, some minor topological alterations such as surface deformations were seen until it reached zone III (70-145 Jcm^{-2}) where the signs of melting were clearly observed and it gradually became stronger. This is consistent with the fact that the power density required for melting (I_m) most metals is in the order of 10^5 Wcm^{-2} which in this case the corresponding range would be between 365-725 $kWcm^{-2}$. It is however, important to notice from metallurgical point of view that melting initially begins due to temperature rise of different elements at the surface. Hence, gradually these island-type molten centers are joined together producing a larger molten pool. Finally, zone IV (145 Jcm^{-2}-above) represents the onset of gradual thermal ablation (vis.vapourization) of Ti6Al4V at $\geq$145 Jcm^{-2} with corresponding temperature of about 3280(°c). Normally this process is accompanied by the presence of plume which basically is defined as ejection of material from the metal surface as gaseous and solid phase particles. Again this behaviour is expected to become dominant with vaporization intensity threshold of about 10^6 Wcm^{-2}.It is deduced from Fig. 7 that "Incubation" effect or period can be observed at lower fluences where more laser pulses may be needed in order to reach the ablation threshold. It may be worth while to notice that this

effect had also been observed and reported for polymers by other investigators [Srinivassan et al., 1990; Dyer & Karnakis, 1994]. Also to avoid possible errors in assessment and evaluation of interaction process a distinction must be made between the actual physical ablation and surface non-linear roughness (ie. ripples) even occasionally with relatively high amplitudes which in our case this began at about 30 Jcm-2. The etch depth saturation became particularly noticeable at higher fluences, which is mainly thought to be due to an intense interaction between the laser pulse and laser-induced vapor plume, hence causing some effective beam attenuation.
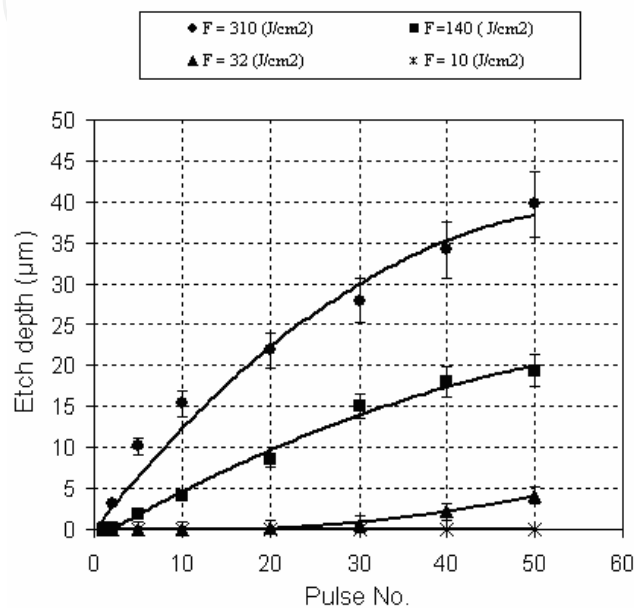
Fig. 7. Variation of etch depth as a function of laser pulse number at constant laser fluences

Since in our experiment the pulse duration is much greater than the thermal relaxation time (i.e. $\tau \approx 200\ \mu s \gg \tau_r \approx \alpha^{-2}/4k \approx 140$ ns) and that the optical absorption depth, α^{-1}, is much smaller than thermal diffusion depth, z_t, (i.e. $\alpha^{-1} \approx 2\mu m \ll z_t \approx 2(k\tau_p)^{1/2} \approx 7.5$ mm) thus, the temperature rise at the end of laser pulse on the surface is given by equation 7:

$$T_f - T_i = \frac{(1-R)F}{\rho c \left(4 k \tau_p\right)^{\frac{1}{2}}} \tag{7}$$

With [Ifflander, 2001]:

- T_f, T_i = final and initial surface temperature (°c).
- R = surface reflection (0.6)
- C = specific heat capacity (0.52Jg-1°c-1)
- ρ = density (4.51gcm-3)
- k = diffusivity coefficient (0.07cm2s-1)
- τ_p = pulse width (200μs)

Fig. 8 indicates the variation of Ti6Al4V surface temperature as a function of laser fluence. Now by assuming the melting and vaporization points of Ti6Al4V about 1668°C and 3280°C respectively and the melting region between (73-145) Jcm-2, using Fig. 6, then it would be sensible to choose zone III as the treatment area (ie. below ablation).
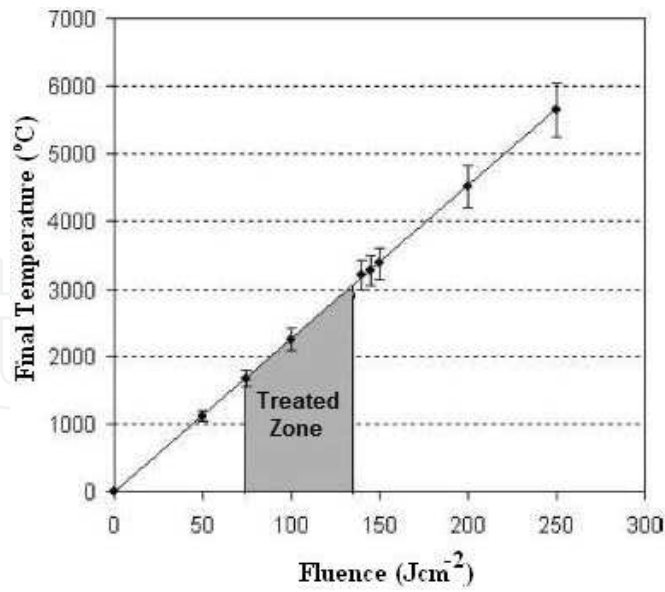
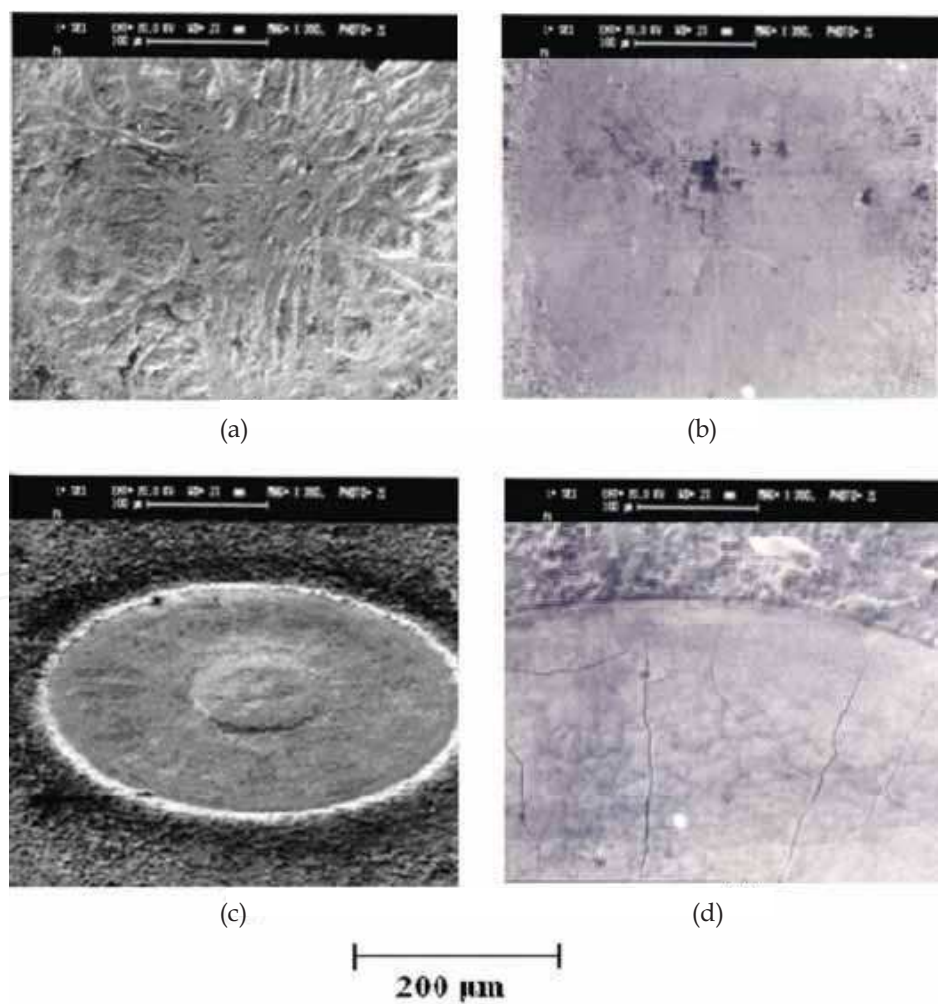Fig. 8. Plot of Ti6Al4V surface temperature versus laser fluence

(a)   (b)

(c)   (d)

|————— 200 μm —————|

Fig. 9. Surface morphology of Ti6Al4V treated at a) 100 Jcm⁻² b) 140 Jcm⁻² c) 210 Jcm⁻² d) Crack formation at Ti6Al4V surface after 10 pulses treated at 270 Jcm⁻²

The comparison between morphologically different textures produced by laser at different energy density is shown in Fig. 9. Fig. 9a indicates the interaction effect and the pattern of dentritic melted zone at 100Jcm^{-2}. It is known that as the growth rate of solid phase increases with time during solidification process, the morphology of liquid / solid interface changes from planar to dentritic structure.These random fluctuating dentritic features are in turn defined by dentritc tip radius and their spacing between them [Dreyfus, 1992]. When the laser fluence was increased to 140Jcm^{-2}, the thermal ablation became the dominant mechanism where the irregularities and scratches due to machining and polishing process became smooth after direct laser surface thermal processing, Fig. 9b. Fig. 9c indicates the difference between the untreated and treated surface at 210Jcm^{-2} with formation of some grainy structure and cracks in cellular form in the central zone. Finally when the fluence was increased to 270Jcm^{-2} (Fig. 9d) these cracks became dominant and developed throughout the surface caused by residual mechanical stress originated from steep temperature gradients at the surface during the resolidification process.

Fig. 10 shows an example of the ablation site at fluence of ≥ 250 Jcm^{-2} (i.e. I >1mWcm^{-2}) with 10 pulses which has caused the metal eruption, cracks as well as surface melting. The spectra of colors, mainly blue, are probably because of high temperature plasma roughly defined by $T_e = C.(P\lambda\sqrt{\tau_p})^{1/2}$ where C is a material depending constant, T_e is electrons temperature, P and λ are the laser power and wavelength respectively [Majumdar & Manna, 2003]. Also, other factors like surface composition, solubility degree of alloys and base metal, thermal diffusion and rate of heating-cooling cycle may all have specific roles in crack formation which need a separate attention and analysis.
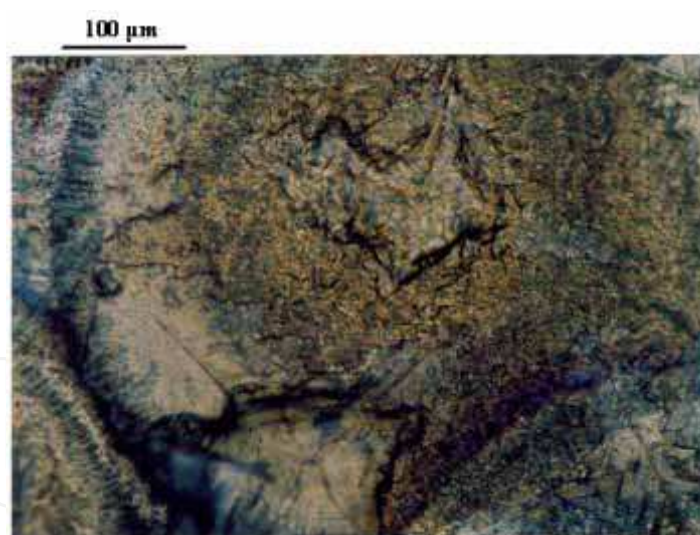

Fig. 10. Plasma –induced damage of titanium at 250 Jcm^{-2} with 10 pulses

Two morphologically different areas i.e. laser treated and untreated (Fig. 11) indicate that the inclusions are disappeared and the scratches due to machining and polishing are sealed due to direct laser surface heating. Ti6Al4V alloy is a (α+β) two-phase alloy with around 6wt% aluminum stabilizing the phase and about 4wt% vanadium stabilizing the β phase. At room temperature, the microstructure at equilibrium consists mainly of primary a phase (hcp) with some retained β phase (bcc). It is also well known that in laser surface melting, steep temperature gradient and thermal cycle leads to some micro structural changes in the heat affected zone within very short time. In particular, the α + β phase transformation

during rapid heating and decomposition of the β phase during rapid cooling. The physical and mechanical properties of Ti6Al4V alloy are known to be sensitive to its microstructure. The Ti-β phase has a diffusivity of two orders of magnitude higher than Ti-α phase and flow stress is strongly influenced by the ratio of these phases [Fan et al., 2005].
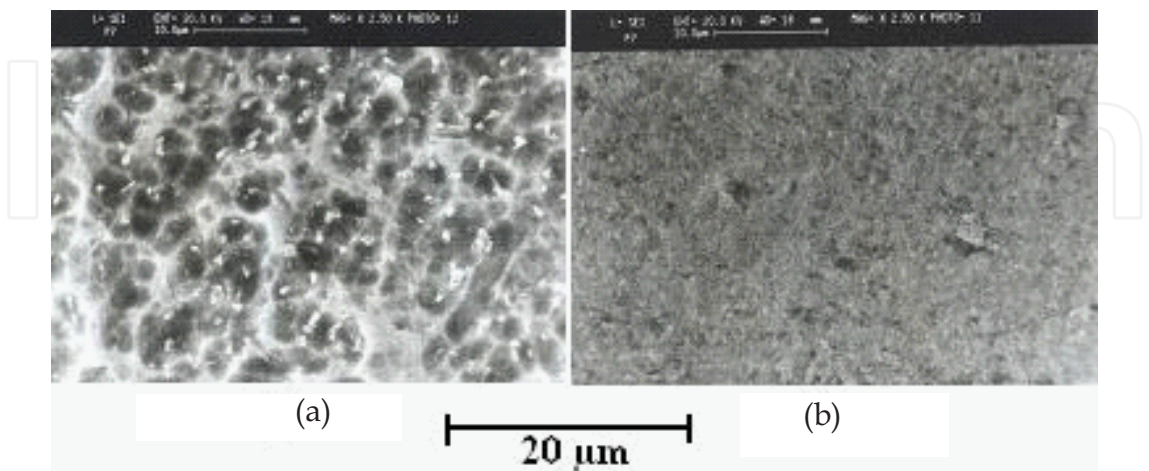

(a)   20 μm   (b)

Fig. 11. Scanning electron micrographs of Ti6Al4V surface morphology for: (a) untreated, (b) laser treated at 140 Jcm^{-2} indicating the disappearing of surface scratches by laser surface melting

Surface Roughness

In order to obtain a quantitative comparison between the original and treated surface, the arithmetic average of the absolute values of all points of profile (R_a) was calculated for all samples. A value of 7±0.02 was obtained for laser treated surface at 140 Jcm^{-2}. Also the R_a values for untreated and laser treated at 100 Jcm^{-2} were 12.3±0.03 and 14.2±0.29 respectively. All the calculations were performed for n=5 and reported as a mean value of standard deviation (SD).
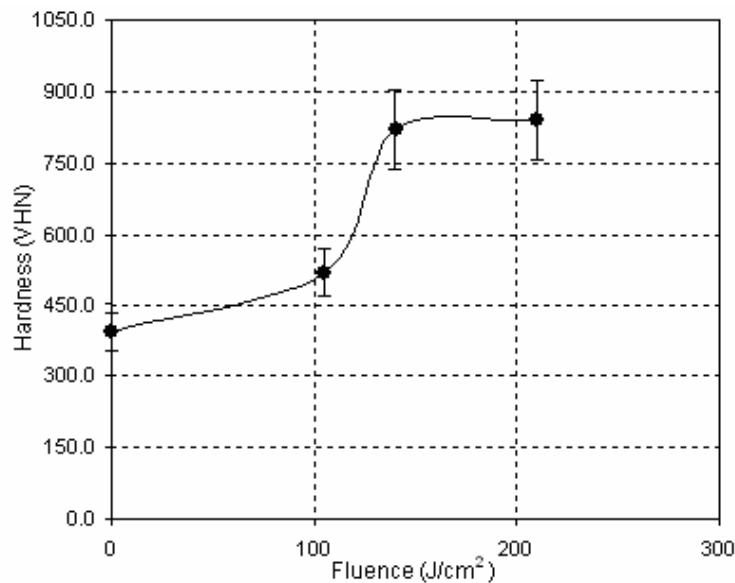
Surface Hardness

Fig. 12. Variation of surface hardness with fluence

Characterization and Evaluation of Surface Modified Titanium Alloy
by Long Pulse Nd:YAG Laser for Orthopaedic Applications: An *Invivo* Study
187

The surface hardness measurements presented in Fig. 12 clearly indicate that micro hardness of the metal increases with laser fluence. Again a non-linear behaviour was observed where initially the values of VHN were increased gradually up to about 100 Jcm^{-2}. Afterwards a sharp increase occurred until the point of plateau was reached at 140 Jcm^{-2} which corresponds to roughly 50% improvement of surface hardness. The surface hardness was found to vary from 377 VHN for MTS to 850 VHN for LTS.

The surface hardness results for all the specimens are illustrated in table 2.

Sample	Microhardness (HVN)
Untreated	394
140 Jcm^{-2}	850

Table 2. Surface hardness tests before and after treatment

EDX analysis

The experimental results of EDX spectroscopy of the untreated and treated samples in the ambient condition is given in Fig. 13. The analysis exhibited K-α lines for aluminium and titanium for both samples, though it was expected carbon to be detected too. It is seen from Fig. 14 that as the laser fluence was increased, the vanadium percent showed a decreasing trend until it reached to its maximum reduced value at about 145Jcm^{-2} where there onwards it was increased again. Perhaps from biomedical applications point of view a better and safer cell attachment and growth can be expected in above condition since surface toxicity has reduced even further. Table 3 indicates the differences in surface elements after treating by laser irradiation.
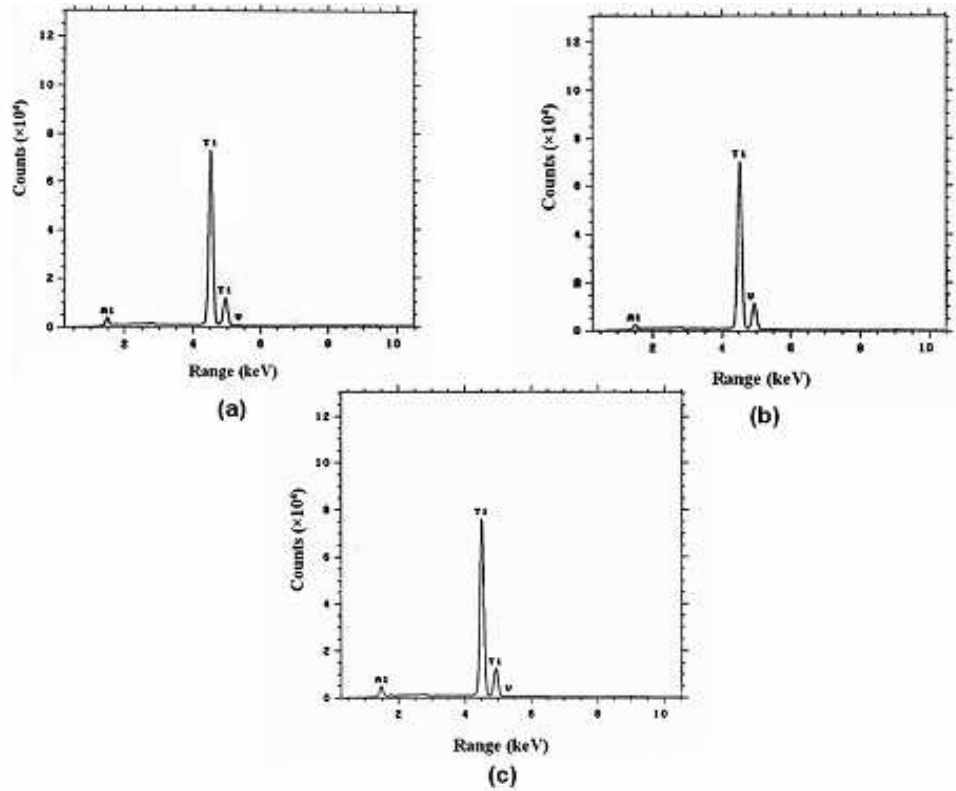

Fig. 13. EDXA analysis of the implant surface, a) untreated b) treated at 100 Jcm^{-2} c)treated at 140 Jcm^{-2}
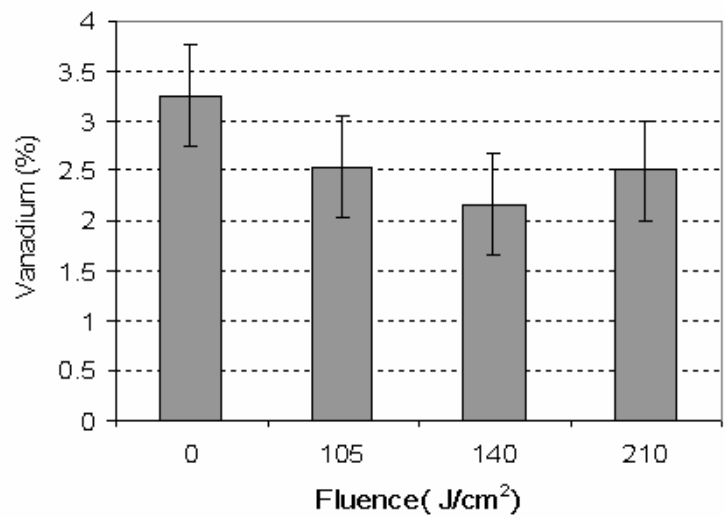
Fig. 14. Changes of Vanadium at the alloy surface as a function of fluence

Element sample	%Al	%V	%Ti
Untreated	5.15	3.25	91.6
140 Jcm^{-2}	3.96	2.54	93.5

Table 3. Surface elements composition before and after treatment

Corrosion test

The comparison of these curves indicates a few important points:1-a value of 1.77×10^{-3} mpy for untreated sample (Fig. 15a), 2- the corrosion rate for laser treated specimen reduced to 0.46×10^{-3} mpy at 140 Jcm^{-2} (Fig. 15b), 3- E_{corr} varied from -0.51 V to -0.21 V after the treatment at 140 Jcm^{-2}. This means that the laser treated specimen is placed at a higher position in the cathodic section of the curve hence releasing hydrogen easier and acts as an electron donor to electrolyte. Therefore, by smoothly reaching the passivation region, a more noble metal is expected to be achieved. The corrosion current (I_{corr}) was decreased from 2.54 µAcm^{-2} to 0.66 µAcm^{-2} after surface laser treatment which can imply a better corrosion resistance.

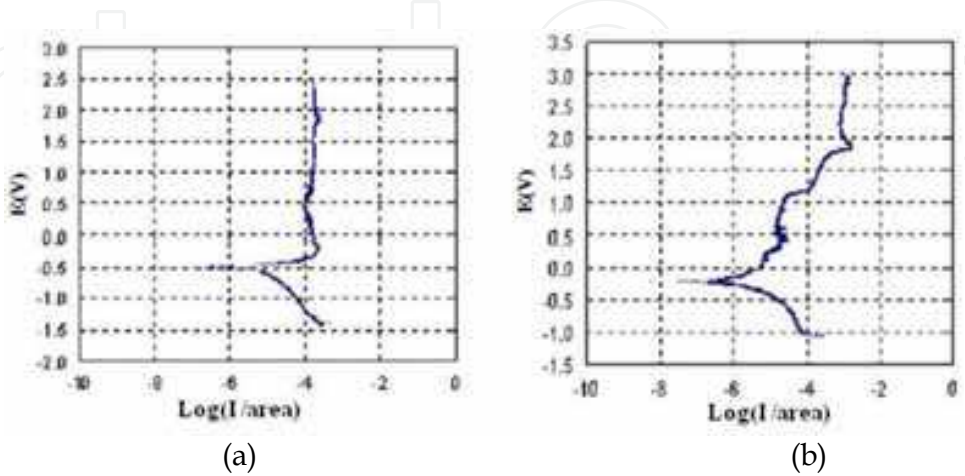(a)   (b)

Fig. 15. Tafel potentiodynamic polarization curves of Ti6Al4V for: (a) untreated, (b) at 140 Jcm^{-2}

Surface tension

The change in surface wettability was studied by contact angle measurement for all specimens treated at 100 Jcm^{-2}, 140 Jcm^{-2} (Fig. 16a). A smoother surface was achieved by laser radiation at 140 Jcm^{-2} which means a reduction in contact angle. This effectively implies an increase in degree of wettability of the metal surface. It is, however, important to note that a smoother surface and enhanced oxygen content, which depends on oxide layer thickness, can both help to reduce the contact angle. This is so because the surfaces with higher concentration of oxygen atoms and more incorporation of oxygen-base polar functionalities of surface exhibit higher wettability (ie. lower contact angle) hence an improvement of biocompatibility, though some believe that, hydrophilicity alone is an inadequate promoter of cell adhesion and retention [Baier et al., 1984]. As a result, it is emphasized that a better cell adhesion can be obtained for the specimens with apparently higher surface energy, rather than higher surface roughness.

According to primary melting centers topology, the surface roughness was increased slightly at 100 Jcm^{-2} (R_a =14.2 ± 0.29). Thus an increase of contact angle occurs from 70° to 80° indicating a lower degree of wettability. Following the laser treatment at 140 Jcm^{-2} the contact angle reduced to 37 ^{o} showing still a more acceptable hydrophilic behaviour. Also, variation of surface tension for all specimens was calculated by measured contact angle. It is known that as contact angle decreases, the related surface tension will be increased. Therefore, a value of 58mN/m was obtained for γ at 140 Jcm^{-2} which is considerably higher than 39mN/m of the untreated sample. The corresponding values of γ for 100 Jcm^{-2} were found as 31mN/m (Fig. 16b).
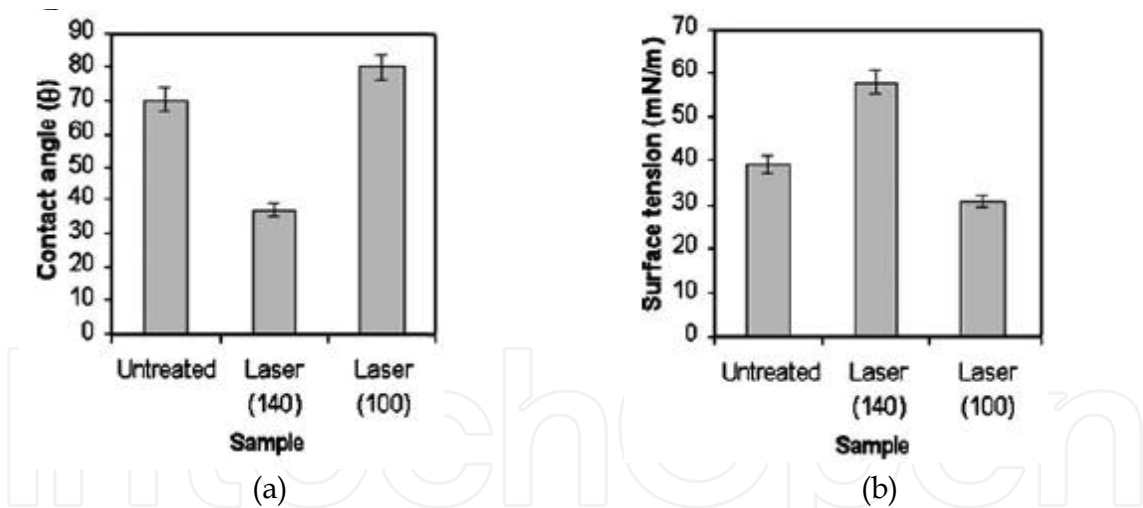

Fig. 16. Variation of contact angle: (a) and surface tension, (b) with sample surface texture

In vivo
Cell spreading analysis

The experimental results of bone cell growth are given in table 4. As it can be seen, cells spreading over the specimen surface is related to laser fluence and surface texture which was measured by Image J program software (IJP). The highest spreading area (488 μm^2) belongs to the LTS at 140 Jcm^{-2}.

The SEM analysis of attached cells morphology (Fig. 17) indicates that the density of cell network is directly dependent on the laser beam fluence and surface topography. The smooth surface produced at 140 Jcm^{-2} not only caused a dense cell network but also resulted

in a wider area covered by a single cell spreading. Density of network is originated from monolayer attachment (cell-surface) change to multilayer (cell-surface & cell-cell). As it is seen no specific directional spread of attached cells was achieved in laser treated specimens.

Row	Specimens	Spread cell area (μm^2)
1	untreated	352 ± 6
2	100 (Jcm^{-2})	316± 10
3	140 (Jcm^{-2})	488 ± 8

Table 4. Bone cells spread over the surface of the implanted specimens (average of ten measurements in three separate regions)
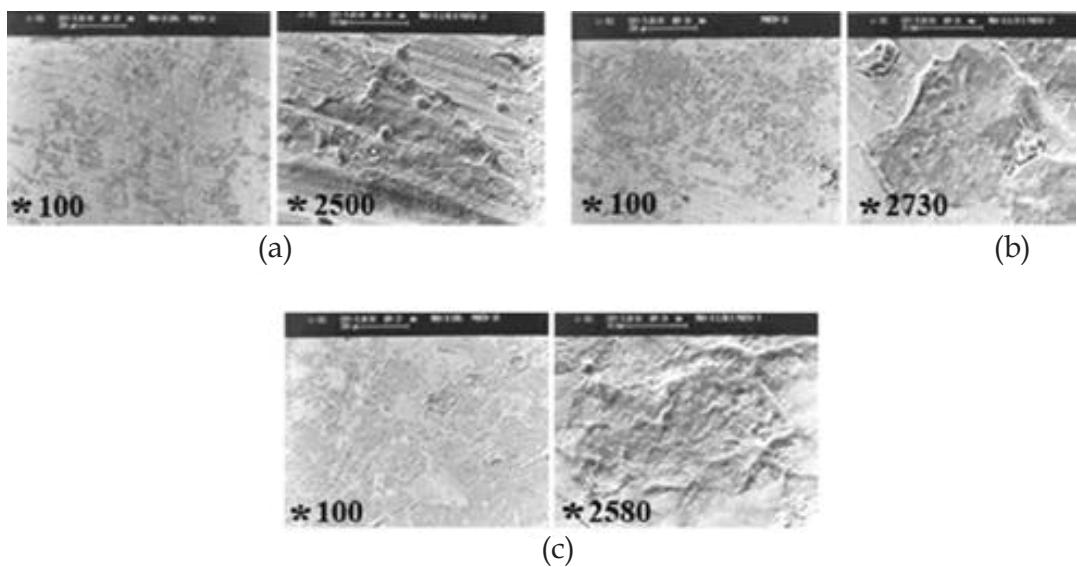

(a)   (b)

(c)

Fig. 17. Scanning electron micrographs of attached cells on the surface for: (a) untreated, (b) at 100 Jcm^{-2}, (c) at 140 Jcm^{-2}
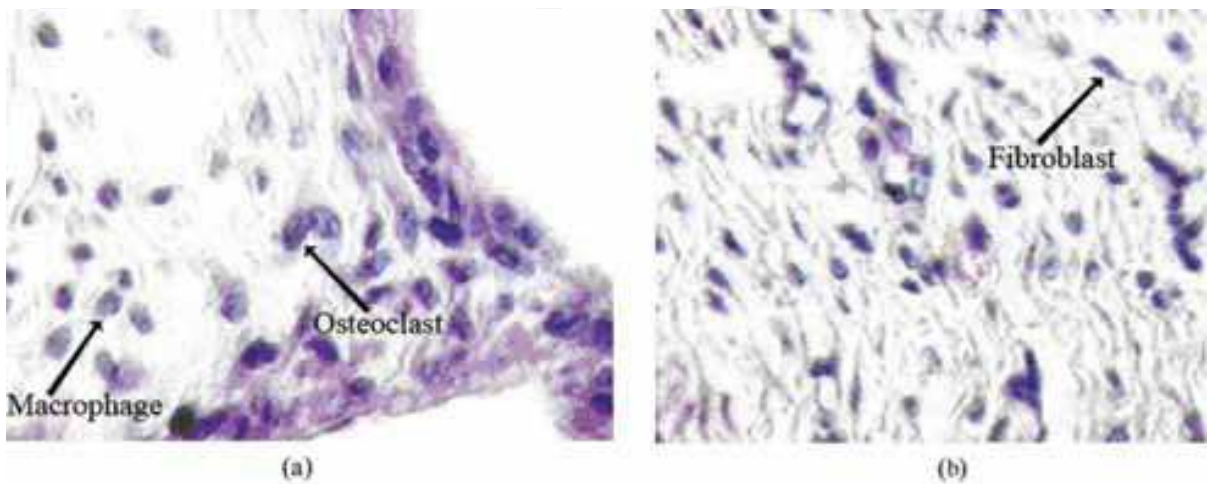
Histopathology

(a)   (b)

Fig. 18. Light microscopy evaluation of bone tissue for: (a) untreated, (b) samples laser treated at 140 Jcm^{-2}

Characterization and Evaluation of Surface Modified Titanium Alloy
by Long Pulse Nd:YAG Laser for Orthopaedic Applications: An *Invivo* Study
191

When the implants were retrieved, no inflammatory reaction was observed inside or around the implants. Mineralized matrix deposition and bone cells were observed on the surface of implants which are formed during the five months implantation. This deposition was found all around of LTS (Fig. 18b) and bone formation was characterized by the occurrence of osteocyte embedded in the matrix. Also the above samples were surrounded by fibroblast and osteoblast cells and the untreated sample (Fig. 18a) showed not only less number of fibroblast cells, also contained osteoclast and polymorpho nuclear leukocytes (PMN).

As it is seen from Fig. 19 the bone tissue nutrition is carried out through the channel in LTS where as it was not observed in the case of untreated sample. No PMN, giant cells and osteoclast were seen in laser treated samples at 140 Jcm^{-2}. Also tissue healing was better conducted near mentioned implant rather than all the other evaluated specimens. Fibroblast and osteoblast cells were also numerous at 140Jcm^{-2}.
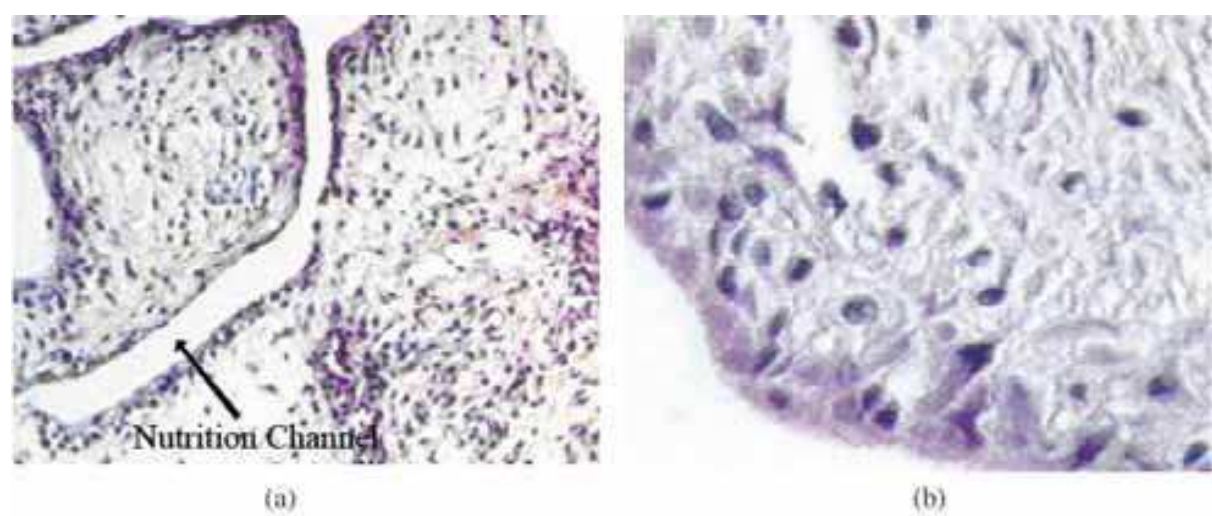

Fig. 19. (a) Light microscopy evaluation of bone tissue for: (a) laser treated sample at 140 Jcm^{-2}, with a nutrition channel shown, and (b) untreated without the channel

In table 5, The symbols indicate the presence of 2-3 cells (+), 3-5 cells (++), more than 5 cells (+++) and lack of cells (-) respectively. No PMN, giant cells and osteoclast were seen in laser treated sample at 140 Jcm^{-2}. Also tissue healing was better conducted near mentioned implant rather than all other evaluated specimens. Fibroblast and osteoblast cells were also numerous in qualitative scales for 140Jcm^{-2} case.

Sample Cell	untreated	100 Jcm^{-2}	140 Jcm^{-2}
Fibroblast	++	+++	+++
Osteoblast	+	++	+++
Giant cell	-	-	-
Osteoclast	+	-	-
PMN	+	+	-
Lymphocyte	++	+++	++
Macrophage	++	+++	++
Healing	+	+	++

Table 5. Qualitative evaluation of histology results of bone tissue around the implants

4. Discussion

The successful incorporation of bone implants strongly depends on a firm longstanding adhesion of the tissue surrounding the implants. The cellular reaction is influenced by the properties of the bulk materials as well as the specifications of the surface, that is, the chemical composition and the topography [Birte et al., 2003; Sikavitsas et al., 2003; Fischer et al., 2004; Peto et al., 2002; Gyorgy et al., 2002]. When one is considering materials for application of orthopaedic implants, it is important to consider a number of factors, such as biocompatibility and surface wettability. The stable oxide layer formed on the implant sample is known to be responsible for the biocompatibility of metal implants. Hence, for a successful laser surface processing of materials some optical and physical parameters must be carefully optimized in order to achieve a desirable surface morphology. It is known that the modification efficiency and the quality is not only the laser fluence dependent but also depend on the spatial and temporal profile of laser beam. Generally the energy absorbed from the laser is assumed to be converted to thermal energy which causes melting, vaporization of the molten material, dissociation or ionization of vaporized material and shock waves in the vapour and the solid. The interaction process was shown to be dependent on the laser fluence, as well as physico-chemical and optical properties of material. Usually, the deposited energy of laser irradiation is converted in to heat on time scale shorter than the pulse duration or laser interaction time. The resulting temperature profile depends on the deposited energy profile and thermal diffusion rate during laser irradiation. Thermal conductivity, K is related to k, ρ and c as follows:

$$K = k\rho c \tag{8}$$

This gives a value of $16 \mathrm{WC^{-1}m^{-1}}$ which is much larger than the optical absorption depth ($\approx 2\mu m$). Therefore, the heat source is essentially a surface source. As it was defined earlier the vertical distance (z_t) over which heat diffuses during the τ_p is about 7.5 mm wher z_t determines the temperature profile. The condition $\alpha^{-1} << z_t$ is typically applicable for laser irradiation of metals. In the present study, a non-adiabatic thermal evaporation was considered as the dominant mechanism during the laser-material interaction process.

A numerical simulation is performed based on date given in before section in order to evaluate the variation of the surface temperature of Ti6Al4V during the heating and cooling cycles. The fundamental Fourier heat transform describing the surface temperature T(x,t) is:

$$\rho c \frac{\partial T(x,t)}{\partial t} - k\nabla^2 T - Q(x,t) = 0 \tag{9}$$
$$0 < x < \infty$$

where ∇ is laplace transform and Q is the heat source.

During heating ($t < \tau_p$), the solution is

$$T(x,t) = T_h(x,t) = \frac{I_0\alpha}{K}\left[\left(\frac{4kt}{\pi}\right)^{\frac{1}{2}}\exp\left(\frac{x^2}{4kt}\right) - x\mathrm{erfc}\frac{x}{(4kt)^{\frac{1}{2}}}\right] + T_0 \tag{10}$$

During cooling the temperature drops for all $t > \tau_p$ and

$$T(x,t) = T_c(x,t) = \frac{I_0\alpha}{K}(4k)^{\frac{1}{2}}\left[\sqrt{t} \times ierfc\frac{x}{(4kt)^{\frac{1}{2}}} - \sqrt{t-\tau_p} \times ierfc\frac{x}{\sqrt{4k(t-\tau_p)}}\right] + T_0 \qquad (11)$$

where i erf(x) is the integral of the complementary error function defined as

$$ierfc(x) = \int_x^\infty erfc(y)dy = \frac{1}{\sqrt{\pi}}e^{-x^2} - xerfc(x) \qquad (12)$$

Equations (10) and (11) have been solven numerically using MATHCAD computer program. Fig. 20 shows the calculated surface temperature variation with the time for the Ti6Al4V irradiated by the pulsed Nd:YAG laser. The followings results can be calculated from the numerical simultion: (i) increasing the laser fluence, increasing the surface temperature, (ii) the numerical results indicate that the maximum µm temperature achieved at the end of the laser pulse in higher than experimental values of melting ($\approx$1668°C) and vaporization (3280°C) temperatures, (iii) almost all the pulse energy at 70 Jcm^{-2} is expended to raise the surface temperature to melting point at the end of its duration (i.e., 200 µs). (iv) consequently, at high fluences, a less time is required to reach the melting point and hence the rest of available time is spent for vaporization and some thermal damage. (v) at higher fluences the temperature gradient become steeper and hence the probability of an unstable front leading to dentritics or crack increases during the cooling cycle.
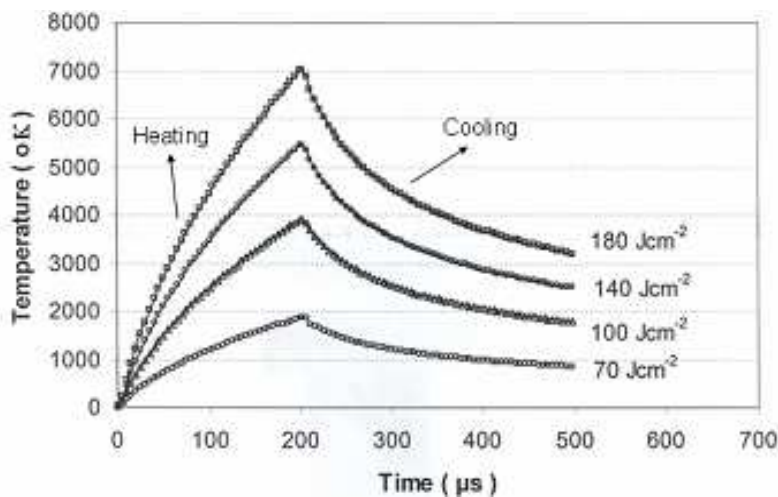

Fig. 20. The surface temperature variation of Ti6Al4V with time

Therefore, selecting a correct energy density for surface treatment has direct influence on the physical properties such as surface microhardness, corrosion resistance, wettability and surface tension of Ti6Al4V. For example, it seems uniformly accepted that any contamination has unfavorable biological effects which may catalyze oxidation, hence it may enhance the dissolution of Ti ions from implant surface. With this view, it is suggested [Joob-Fancsaly, 2002] that the surface contamination decreases the surface energy of material which is responsible for the surface adsorption of proteins at molecular level.

The contact angle decreased by about 50 percent between 100 Jcm^{-2} and 140 Jcm^{-2} when the surface became smoother It is, however important to notice that the NCLP method cannot measure the topographic features smaller than 1µm which are often found on the roughened

implant surface due to its resolving power limitation. Also, a superior microhardness value was exhibited by the sample which can be attributed to grain refinement associated with laser melting and rapid solidification.

Generally a change in the corrosion potential (E_{corr}) indicates a microstructural modification in the metal. For this purpose the Tafel potentiodynamic polarization experiments were performed on Ti6Al4V in Hank's salt balanced physiological solution for untreated, laser treated, see Fig. 15. Also, an increase of corrosion resistance by about 74% which is mainly thought to be due to removal of surface inclusions and surface micro-smoothing during the laser treatment possibly caused by the lateral flow of molten material due to surface tension. Practiclly this means that the laser treated specimen is placed at a higher position in the cathodic section of the curve hence releasing hydrogen easier and acts as an electron donor to electrolyte. Therefore, by smoothly reaching the passivation region, a more noble metal is expected to be achieved which should be more impermeable and resistant to corrosion. This effect was observed within zone III (Fig. 6), where the surface melting was set at about 70 Jcm^{-2}. Among the possible involved mechanisms controlling the hydrodynamics of the melt region is its displacement resulting from the local pressure applied to the liquid surface as a result of the evaporation process. In this range, surface porosities and irregularities of untreated sample became almost completely sealed, Fig. 9b, and the roughness was reduced. Treatment at fluence of 140 Jcm^{-2} with 10 pulses produced optimum effects on the surface. However, at higher fluences in zone IV, even though melting and vaporization are both at work, the surface roughness mainly defined by grainy structure, meandering , cell boundaries, and the cracks were increased, Fig. 9d. This effect may be resulted from reduced thermal accumulation on the metal surface by blasting off the sealed layer hence, causing the increase of local roughness. The grains, surface cooling rate after laser treatment, heat transfer from lower or lateral metal layer and short time duration between heating and cooling cycle may all cause some changes in remaining β phase shape. In addition to surface morphology, the properties of implant materials affect cellular behaviour such as wettability. The wettability of the surface plays an important role with respect to protein adsorption, cell attachment and spreading. It is known that surfaces with high surface free energy are to be more adhesive than those with a low surface free energy. In this study the values for surface free energy showed significant differences between laser treated, untreated sample.

It is also worth to notice that all the samples were treated in an ambient condition and were steam sterilized which would have a great influence on surface composition of Ti especially in TiO$_2$ formation. It is proved that the samples irradiated by laser beam during the treatment can cause oxygen diffusion through the molten materials and thus to oxidize the titanium [Perez del Pino et al., 2002]. Also the variation of surface oxidation layer thickness depends on steam sterilization process and the time of exposure to air [Sitting et al., 2000]. As the oxygen content of surface increases, the measured contact angle decreases. This is explained by the fact that surfaces with higher concentration of oxygen atoms and more incorporation of oxygen-base polar functionalities of surface exhibit higher wettability (lower contact angle). The local presence of the alloying elements Al and V within the passive oxide film is likely to influence the adsorption of proteins and their conformation on the surface which in turn is expected to modify cell-surface interaction. If cells are affected by the presence of hydroxides on the surface, then developing an understanding of the mechanisms that control this interaction could lead to the optimization of this parameter in

Characterization and Evaluation of Surface Modified Titanium Alloy
by Long Pulse Nd:YAG Laser for Orthopaedic Applications: An *Invivo* Study
195

current and future metallic biomaterials [Bern et al., 2004]. Also, other factors like surface composition, solubility degree of alloys and base metal, thermal diffusion and heating/cooling rate may have a specific role in crack formation which needs a separate attention and analysis.

The interaction of living cells with foreign materials is complicated matter, but fundamental for biology medicine and is a key for understanding the biocompatibility. The initial cellular events which take place at the biomaterials interface mimic to a certain extent the natural adhesive interaction of cells with the extra cellular matrix (ECM). The osteoblasts, which play a principal role in bone formation, readily attach to the material surfaces via adsorbed protein layer consisting or RGD containing ligands like fibronectin, vitronectin or fibrinogen. Family of cell surface receptors that provide trans- membrane links between the ECM and the cytoskeleton. The focal point in laser treated surface at 140 Jcm-2 should be approximately 10 nm which is convenient for bone cells to get close enough to be activated and attach to the surface in order to form an extra cellular matrix. In this state, bone cells will spread over the smooth surface much more easily and fluently.

Our study showed that surface micro grooves can affect the orientation guidance of bone cells i.e. the deeper grooves were more effective in guiding the cells as it was evaluated by SEM. However, we did not conduct or evaluate systematically the exact effects of grooves depth and size on cell orientation, but our preliminary results were similar to those reported by Xiong & Yang, 2003. It seems, however, that laser treated surface did not regulate the cells shape exactly similar to other investigations. The finding of most research works that the osteoblast cells grow slightly better on the rougher surface indicate the fact the surface topography indeed affects the osteoblast cell proliferation. However, our results showed that laser treated samples at 140 Jcm-2 produced a smoother and higher wettability characteristics than the mechanically roughend surface. This finding agrees with Hao[a] et al., 2005 and Mirhosseini et al., 2007 works where they found similar results with Ti6Al4V using diode laser. It is, believed that oxygen content of material surface can contribute to the improvement of the wettability characteristics in laser surface modification. It is also equally important from our point of view to carefully distinguish and discuss the difference between the mechanism of cell attachment on a rough surface and cell adhesivity on a smooth surface and their impacts on biomedical engineering [Hao[a] et al., 2005, Hao[b] et al., 2005].

5. Conclusion

This study was focused on the topographic effects of Ti6Al4V produced by laser radiation on goat bone cell adhesion. The results showed a common feature reported in the previous studies on a variety of cell types and substrates ie, topographic features strongly affects the cell guidance. We found a significant difference when comparing the cells behaviour on unevenly micro grooves and smooth surfaces. This study shows that a smooth surface can exhibit more cell adhesivity compared with micro grooved surface due to its increase of surface tension and reduction of contact angle and probably the presence of oxygen content at the surface. The test confirmed that the highest number of cells are attached to the LTS at 140 Jcm-2. It is also concluded from the SEM, contact angle measurements and preliminary *in vitro* and *in vivo* tests that Nd:YAG laser can induce a desirable surface modification on Ti6Al4V alloy for cell adhesivity and that a noble and biocompatible Ti alloy with better

physico–chemical properties can be obtained under suitably defined optical condition. Finally it is suggested that more detailed experiments are required and would be useful to distinguish and clarify the difference between attachment on the rough surface via physical anchoring and adhesion on smooth surface by chemical binding. Also, the relation between the grooves size and their orientation must be studied more carefully with respect to cell attachment and their reliability as well as endurance.

6. References

Albrektsson, T.; Branemark, P.I.; Hansson, B.O. & Lindstrom, J. (1981). Osseointegrated titanium implants. *Acta Orthop. Scand,* 52, 155-170

Albrektsson, T. & Johansson, C. (2001). Osteoinduction, osteoconduction and osseointegration. *Eur. Spine. J*, 10, 96-101

Anselme, K.; Linez, P.; Bigeralle, M.; Maguer, D.L.; Maguer, A.L.; Hardouin, P.; Hildebrand,H.F.; Iost, A. & Leroy, J. M. (2000). The relative influence of the topography and chemistry of Ti-6A1-4V surfaces on osteoblastic cell behaviour. *Biomaterials*, 21, 1567-1577

Aparicio, C.; Javier, F.; Fonceca, C.; Barbosa, M. & planell, J. A. (2003). Corrosion behaviorof commercially pure titanium shot blasted with different material and sizes of shot particles for dental implant applications. *Biomaterials*, 24, 263-273

Arisu, H.D.; Turkoz, E. & Bala, O. (2006). Effects of Nd:YAG laser irradiation on osteoblast cell cultures. *Laser in Medical Sci.*, 21, 175-180

Assmann, W.; Schubert, M.; Held, A.; Pichler, A.; Chill, A.; Kiermaier, S.; Schlösser, K.; Busch, H.; Schenk, K. & Streufert, D. (2007). Biodegradable radioactive implants for glaucoma filtering surgery produced by ion implantation. *Nucl. Inst. and Methods. In phys. Res. Sec.B*, 257,108-113

Baier, R.E ; Meyer, A.E. ; Natiella, J.R. ; Natiella R.R. & Carter, J.M. (1984). Surface properties determine bioadhesive out comes: methods and results. *J Biomed. Mater. Res.*, 18, 337-355

Beraceras, I.; Alava, I.; Onate, J.I. & Maezto, M.A. (2002). Improved osseointegration in ion implantation-treated dental implants. *Surf. & Coat. Tech.*, 158-159, 28-36.

Birte, G.S.; Neubert, A.; Hopp, M.; Griepentrog, M. & Lange, K.P. (2003). Fibroblast growth on surface modified dental implants: An in vitro study. *J Biomed. Mater. Res. 64A,*591-599

Bigerelle, M. & Anselme, K. (2005). Bootstrap analysis of the relation between initial adhesive events and long-term cellular functions of human osteoblasts cultured onbiocompatible metallic substrates. *Acta biomaterialia,*1, 499-510

Branemark, P.I.; Hansson, B.O.; Adell, R. & et al. (1977). Osseointegrated implants in the treatment of the edentulous jaw. *Scand. J Plastic recounst. Surg. Suppl.*, 16, 1-116

Breme, H. J. & Helsen, J.A. (1998). Metals as Biomaterials, West Sussex:wiley, 30-70

Brunette, D.M. & Cheroudi, B. (1999). The effect of topography of micromachined titaniumsubstrate on cell behaviour in vitro and invivo. *J Biomech. Eng.*, 121, 49-57

Buchter, A.; Kleinheinz, J.; Wiesman, H.P.; Kersken, J.; Nienkemper, M.; Weyhrother, H.; Joos, U. & Meyer, U. (2005). Biological and biomechanical evaluation of bone remodeling and implant stability after using an ostetome technique. *Clin. Oral Implants Res.*, 1, 1-8

Buchter, A.; Joos, U.; Wiessman, H.P.; Seper, L. & Meyer, U. (2006). Biological andbiomechanical evaluation of interface reaction at conical screw-type implant. *Head and Face Med.*, 2, 5-18

Burser, D. & Schenk, R.K. (1991). Influence of surface characteristics on bone integration of titanium implants. A histomorphometric study in miniature pigs. *J Biomed. Mat. Res.*, 25, 889-902

Bern, L.; English, L.; Fogarty, J.; Policoro, R.; Zsidi, A.; Vance, J.; Drelich, J.; White, C.; Dunahu, S. & Rohly, K. (2004). Effect of surface characteristics of metallic biomaterials on interaction with osteoblast cells.7th World Biomat. Cong., 1121-1122

Cheroudi, B.; Soorany, E.; Black, N. & Weston, L. (1995). Computer-assisted 3D reconstruction of epithelial cells attached to percutaneous implant. *J Biomed. Mater. Res.*, 29, 371-379

Chung, T.; Liu, D. & Wang, S. (2003). Enhancement of the growth of human endothelial cells by surface roughness at nanometer scale. *Biomaterials*, 24, 4655-4661

Cooper, L. F.; Masuda, T.; Yliheikkila, P.K. & Felton, D. A. (1998). Generolization regardingthe process and phenomena of osseointegration, part II. *Int. J Oral Maxillofac. Implants*, 13, 163 -174

Curtis, A.S. & Wilkinson, C.D. (1998). Reaction of cells to topography. *J Biomat. Sci. Polymer Ed.*, 9, 1311-1324

Curtis, A.S. & Clark, P. (2001). The effect of topographic and mechanical properties of materials on cell behaviour. *Crit. Rev. Biocompat.*, 9, 1313-1329

Darvell, B.W.; Samman, N & Luk, W.K. (1995). Contamination of titanium casting by aluminium oxid blasting. *J Detistry*, 23, 319-322

Davies, J.E. (1996). In vitro modeling of the bone implant interface. *Anatomical Recorded*, 245, 426- 445

Deka, B.; Dyer, P.E. & Sayers, J. (1980). Investigation of laser supported detonation waves and thermal coupling 2.8 μm laser irradiated metal targets. *J De Physique*, 41, C9-75

Deppe, H.; Warmuth, S.; Heinrich, A. & Korner, T. (2005). Laser- assisted three dimensional surface modifications of titanium implants: preliminary data. *Laser in Med. Sci.*, 19, 229-233

Dreyfus, R.W. (1992). Comparison of the ablation of dielectrics and metals at high and low laser Powers. In: Fogarassy, E and Lazare, S(eds). *Laser Ablation of elrctronic materials. NewYork Elsevier science*, 61-68

Ducheyne, P. & El-Ghannam, A. (1994). Effect of bioactive glass templates on osteoblast proliferation and in vitro synthesis of bone-like tissue. *J Cell Biochem.*, 56, 162-167

Dyer, P.E. & Karnakis, D. (1994). Analysis of UV radiation transport in polymers exhibiting one-photon incubated absorption. *Appl. Phys. A*, 59, 275-279

Eisenbarth, E.; Velten, D. & Breme, J.(2007). Biomimetic implant coatings. *Biomolecul. Eng.*, 24, 27-32

Fan, Y.; Chen, P.; Yao, Y.L.; Yang, Z & Egland, K. (2005). Effect of phase transformations on laser forming of Ti-6Al-4V alloy. *J Appl. Phys.*, 98, 1-10

Fancsaly, A. J.; Divinyi, T.; Fazekas, A.; Daroczi, C.S. & karacs, A. (2002). Pulsed laser–induced micro and nanosized morphology and composition of titanium dental implants. *Smart Mater. Struct.*, 11, 819-824

Feng, B.; Weng, J.; Yang, B.C.; Qu, S.X. & Zhang, X.D. (2003). Characterization of surface oxide films on titanium and adhesion of osteoblast. *Biomaterials*, 24, 4663-4670.

Fischer, P.; Leber, H.; Romano, V.; Webber, H.P. & Glardon, R. (2004). Microstructure of near-infrared pulsed laser dintered titanium samples. *Appl. Phys. A*, A78, 1219-1227

Gaggl, A.; Schultes, G.; Muller, W.D. & Karcher, H. (2000). Scaning electron mircroscopical analysis of laser–treated titanium implant surfaces–acomparative study. *Biomaterials*, 21, 1067-1073

Galvanetto, E.; Galliano, F.P.; Fassati, A. & Borgioli, F. (2002). Corrosion resistance properties of plasma nitrided Ti-6AL-4V alloy in hydrochloric acid solutions. *Corrosion science*, 44, 1593-1606

Geiger, B. & Bershadsky, A. (2001). Assembly and mechanosensory function of focal contacts. *Curr. Opin. Cell Biol.*, 13, 584-592

Ghoo, B.Y.; Keum, Y.T. & Kim, Y.S. (2001). Evaluation of the mechanical properties of welded metal in tailored steel sheet welded by CO_2 laser. *J Mater. Proce. Tech.*, 113, 692-698

Gyorgy, E.; Mihailesco, I.N.; Serra, P. & Morenza, J.L. (2002). Single pulse Nd:YAG laser irradiation of titanium: influence of laser intensity on surface morphology. *Surf. & Coating Tech.* 154, 63-67

Hao[a], L.; Lawerence, J. & Li, L. (2005). The wettability modification of bio-grade stainlesssteel in contact with simulated physiological liquids by the means of laser irradiation. *Appl. Sur. Sci.*, 247, 453-457

Hao[b], L.; Lawerence, J. & Li, L. (2005). Manipulation of the osteoblast response to a Ti-6Al-4V titanium alloy using a high power diode laser. *Appl. Sur. Sci.*, 247, 602-606

Heinrich, A.; Dengler, K.; Koerner, T.; Haczek, C.; Deppe, H. & Stritzker, B. (2008). Laser-modified titanium implants for improved cell adhesion. *Laser in Medical science*, 23, 5-58

Hollander, D.; Walter, M.; Wirtz, T.; Paar, O. & Eril, H. (2005). Structural mechanical and invitro characterization of individually structured Ti-6Al-4V produced by direct laser forming. *Biomaterials*, 27, 955-963

Hsu, R.; Yang, C.; Huang, C. & Chen, Y. (2004). Electrochemical corrosion properties of Ti-6Al-4V implant alloy in the biological environment. Mat. Sci. Eng. A, 380, 100-109.

Hynes, R.O. (2002). Integrins: bidirectional, allosteric signaling machines. *Cell*, 110, 673- 687

Ifflander, R. (2001). Solid State lasers for Materials Processing. Berlin, Springer series in optical sciences

Joob-Fancsaly, A.; Divinyi, T.; Fazekas, A.; Daroczi, C.S.; Karacs, A. & Peto, G. (2002). Pulsed laser-induced micro- and nanosized morphology and composition of titanium dental implants. *Smart. Mater. Struct.*, 11, 819-824

Juliano, D.J.; Saaedra, S. S. & Truskey, G.A. (1993). Effect of the conformation orientation of adsorbed fibronectin on endothelial cell spreading and the strength of adhesion. *J Biomed Mater. Res.*, 27, 1103-1113

Kawaura, H.; Kawahara, H.O.; Nishino, K. & Saito, T. (2002). New surface treatment using shot blast for improving oxidation resistance of Ti-6Al-4V base alloys. *Mate. Sci. & Eng. A*, 329-331, 589-595

Kazatchkine, M.D. & Carreno, M.P. (1988). Activation of the complement system at the interface between blood and artificial surfaces. *Biomaterials, (Ibid)*, 9, 30-35

Kelly, R.G.; Schully, J.R. & Shoesmith, D.W. (2003). Electrochemical Techniques in Corrosion Science and Engineering. *New York:Marcel Dekker Inc.*, 81,240

Characterization and Evaluation of Surface Modified Titanium Alloy
by Long Pulse Nd:YAG Laser for Orthopaedic Applications: An *Invivo* Study

199

Khor, K.A.; Vreeling, A.; Dong, Z.L. & Cheang, P. (1999). Laser treatment of plasma sprayed HA coatings. *Mater. Sci. Eng. A*, 266, 1-8

Khosroshahi, M.E.; Valanejad, A. & Tavakoli, J. (2004). Evaluation of mid-IR laser radiation effect on 316L stainless steel corrosion resistance in physiological solution. *Amirkabir J of Sci. & Tech.*, 15, 107-115

Khosroshahi[a], M.E.; Mahmoodi, M. & Tavakoli, J. (2007). Characterization of Ti-6Al-4V implant surface treated by Nd:YAG laser and emery paper for orthopaedic applications. *Appl. Surf. Sci.*, 253, 8772-8781

Khosroshahi[b], M.E.; Tavakoli, J. & Mahmoodi, M. (2007). Analysis of bioadhesivity of osteoblast on titanium by Nd:YAG laser. *J of Adhesion*, 83, 151-172

Khosroshahi[a], M.E.; Mahmoodi, M.; Saedinasab, H. & Tahriri, M. (2008). Evaluation of mechanical and electrochemical properties of laser surface modified Ti-6AL-4V for biomedical application: in vitro study. *Surf. Eng.*, 24, 209-218

Khosroshahi[b], M.E.; Mahmoodi, M. and Tavakoli, J. & Tahriri, M. (2008). Effect of Nd:YAG laser radiation on Ti6AL4V alloy properties for biomedical application. *J of Laser Applications*, 20, 209-217

Khosroshahi, M.E.; Mahmoodi, M. & Saedinasab, H. (2009). In vitro and in vivo studies of osteoblast cell response to a Ti6A14V surface modified by Nd:YAG laser and silicon carbide paper. *Laser Med. Sci.*, 24, 925-939

Lavose-Valereto, I.C.; Wolynec, S.; Deboni, M.C. & Konig, B.J.R. (2001). In vitro and in vivo biocompatibility testing of Ti-6Al-7Nb alloy with and without plasma- sprayed hydroxyapatite coating. *J Biomed. Mater. Res.*, 58, 727-733

Majumdar, J.D. & Manna, I. (2003). Laser processing of materials. *Sadhana J*, 28, 495-562.

Majumdar, J.D.; Pinkerton, A.; Liu, Z. & Manna, I. (2005). Microstructure characterisation and process optimization of laser assisted rapid fabrication of 316L stainless steel. *Appl. Surf. Sci.*, 247, 320- 373

Masuda, T.; Yliheikkila, P.K.; Felton, D.A. & Cooper, L.F.(1998). Generolization regarding the process and phenomena of osseointegration: in vivo studies, *part I. Int. J Oral Maxillofac. Implants*, 13, 17- 29

Meyer, U.; Szulezewsli, D.H.; Moller, K.; Heide, K. & Jones, D.B. (1993). Attachment kinetics and differentiation of osteoblasts on different biomaterial surfaces. *Cells Mater.*, 3, 129-140

Mirhosseini, N.; Crouse, P.L.; Schmidth, M.J.J. & Garrod, D. (2007). Laser surface micro-texturing of Ti-6Al4V substrates for improved cell integration. *Appl. Sur. Sci.*, 253, 7738-7743

Morra, M.; Cassinelli, C.; Cascardo, G.; Cahalan, P.; Cahalan, L.; Fini, M. & Giardion, R. (2003). Surface engineering of titanium by collagen immobilization. Surface characterization and in vitro and in vivo studies. *Biomaterials*, 24, 4639- 4654

Neff, J.A.; Tresco, P.A. & Caldwell, K.D. (1999). Surface modification for controlled studies of cell-ligand interactions. *Biomaterials*, 20, 2377-2393

Ong, J.L.; Raikar, G.N. & Smoot, T.M. (1997). Properties of calcium phosphate coating before and after exposure to simulated biological fluid. *Biomaterials*, 18, 1271-1275

Perez del Pino, A.; Serra, P. & Morenzo, J.L. (2002). Oxidation of titanium through Nd:YAG laser irradiation. *Appl. Sur. Sci.*, 8129, 1-4

Peto, G.; Karacs, A.; Paszti, Z.; Guczi, L.; Diviny, T. & Joob, A. (2002). Surface treatment of screw shaped titanium dental implants by high intensity laser pulses. *Appl. Sur. Sci.*, 186, 7-13

Peyer, P.; Scherpereel, X.; Berthe, L.; Carboni, C.; Fabbro, R. & Lemaitre, C. (2000). Surface modification induced in 316L steel by laser peening and shot- peening: Influence of pitting corrosion. *Mat. Sci. Eng.*, 280, 294-302

Pierschbacher, M.D. & Ruoslahi, E. (1984). Cell attachment activity of fibronectin can be duplicated by small synthetic fragments of the molecule. *Nature*, 309, 30-33

Puleo, D.A.; Holleran, L.A.; Doremus, R.H. & Bizios, R. (1989). Osteoblast responses to orthopaedic implant materials in vivo. *J Biomed. Mater. Res.*, 25, 11- 23

Ruoslahi, E. & Pierschbacher, M.D. (1987). New perspectives in cell adhesion: RGD and integrins. Science, 238, 491-497

Ruoslahi, E. (1991). Integrins. *J Clin Invest*, 87, 1-5

Ronold[a], H.J. & Ellingsen, J.E. (2002). Effect of micro-roughness produced by TiO_2 blasting-tensile testing of bone attachment by using coin shaped. *Biomaterials*, 23, 4211-219

Ronold[b], H.J. & Ellingsen, J.E. (2002). The use of a coin shaped implant for direct insitu measurment of attachment strenght for osseointegrating biomaterials surface. *Biomaterials*, 23, 2201- 2209

Ronold, H.J.; Lyngstadaas, S.P. & Ellingsen, J.E. (2003). A study on the effect of dual blasting with TiO_2 on titanium implant surfaces on functional attachment in bone. *J Biomed. Mater. Res.*, 67A, 524-530

Shay-Salit, A.; Shushy, M.; Wolfovitz, E.; Yahav, H.; Breviatrio, F.; Dejana, E. & Resnick, N. (2002). VEGF receptor 2 and the adherencs junction as a mechanical transducer in vascular endothelial cells. *Proc, Natl, Acad, Sci U.S.A.*, 99, 9462-9467

Sowden, D. & Schmitz, J.P. (2002). Self-drilling and self-tapping screws in rat bone: an ultra structural study of the implant interface. *J Oral Maxillofac Surg.*, 60, 294-299

Sighvi, R. & Wang, D.I. (1998). Review: Effects of substratum morphology on cell physiology. *Biotech. Bioeng.*, 43, 764-771

Sikavitsas, V.I.; Temenoff, J.S. & Mikos, A.G. (2001). Biomaterials and bone mechano transduction. *Biomaterials*, 22, 2581-2593

Sun, R.L.; Mao, J.F. & Yang, D.Z. (2001). Microstructural characterization of NiCr, BSiC, laser clad layer on titanium alloy substrate. *Surf. & Coat. Technol.*,150, 199-204

Sahin, Y. & Sur, G. (2004). The effect of Al_2O_3 ,TiN and Ti (C,N) based CVD coating on tool wear in maching metal. *Surface & Coating*, 179, 349-355

Slocombe, A.; Taufik, A. & Li, L. (2000). Diod laser ablation machining of 316L stainless steel powder/polymer composite material: effect of powder geometery. *Appl. Surf. Sci.*, 168, 17-20

Srinivassan, R.; Braran, B. & Casey, K. (1990). Nature of "incubation pulse" in the ultraviolet laser ablation of polymethyl methacrylate. *J Appl. Phys.*, 68, 1842-1847

Sikavitsas, V.I.; Dolder, J.; Bancroft, G. & Jansen, J. (2003). Influence of the in vitro culture period on the in vivo performance of cell/titanium bone tissue- engineered constructs using a rat cranial size defect model. *J Biomed. Mater. Res.*, 67A, 944-951

Sitting, C.; Textor, M.; Spencer, N.D.; Wieland, M. & Vallotton, H. (2000). Surface characterization of implant materials c.pTi, Ti-6Al-4V band Ti-6Al-4V with different pretreatments. *J Mater. Sci.*, 10, 35-46

Characterization and Evaluation of Surface Modified Titanium Alloy
by Long Pulse Nd:YAG Laser for Orthopaedic Applications: An *Invivo* Study
201

Tan, L.; Dodd, R. & Crane, W. (2003). Corrosion and wear- corrosion behaviour of NiTi modified by plasma source ion implatation. *Biomaterials*, 24, 3931- 3939

Tian, Y.S; Chen, C.Z.; Lee, S.T. & Huo, Q.H. (2005). Research progress on laser surface modification of titanium alloys. *Appl. Surf. Sci.*, 242, 177-184

Tirrell, M.; Kokkoli, E. & Biesalski, M. (2002). The role of surface science in bioengineered materials. *Surf. Sci.*, 500, 61-63

Thomas, C.H.; McFarland, C.D.; Jenkins, M.L. & Rezania, A. (1997). The role of vitronectin in the attachment and spatial distribution of bone-drived cells on materials with patterned surface chemistry. *J Bomed. Mater. Res.*, 37, 81- 93

Toth, C.; Szobo, G.; Kovacs, L.; Vargha, K.; Barabas, J. & Nemeth, Z. (2002). Titanium implants with oxidized surfaces: the background and long–term results. *Smart Mater. Stru.*, 11, 813-818

Tian, Y.S.; Chen, C.Z.; Yue, T.M. & Wang, Z.L. (2004). Study on microstructures and mechanical properties of in-situ formed multiphase coating by laser cladding of titanium alloy with silicon and graphite powder. Chin. *J Laser*, 31, 1-12

Tritca, S.; Gakovic, M.; Nenadovic, M. & Mitrovic, M. (2001) Surface modification of stainless steel by TEA CO_2 laser. *Appl. Surf. Sci.*, 177, 48-57

Tritca, M.S.; Tarasenko, V.; Gakovic, B. & Fedenev, A. (2005). Surface modification of TiN coating by pulsed TEA CO_2 and XeCl lasers. *Appl. Sur. Sci.*, 252, 474-482

Trtica, M.S.; Radak, B.B.; Gakovic, B. M.; Milovanovic, D.S.; Batani, D. & Desai, T. (2009). Surface modifications of Ti6A14V by a picosecond Nd:YAG Laser. *Laser and particle Beams*, 27, 85-90

Turner, M.W.; Crouse, P.L. & Li, L. (2007). Comparative interaction mechanisms for different laser systems with selected materials on titanium alloys. *Appl. Surf. Sci.*, 253, 7992-7997

Venugopalan, R.; Weimer, J.J.; George, M.A. & Lucas, L. C. (2000). The effect of nitrogen diffusion hardening on the surface chemistry and scratch resistance of Ti-6AL-4V alloy. *Biomaterials*, 21, 1669-1677

Vercaigne, S.; Wolk, J. & Jansen, J. (1998). The effect of titanium plasma-sprayed implants on trabecular bone healing in the goat. *Biomaterials*, 19, 1093-1099

Vorobyev, A. Y. & Guo, Ch (2007). Femtosecond laser structuring of titanium implants, *Appl. Surf. Sci.*, 253 (17), 7272-7280

Wang, X.X.; Yan, W.; Hayakawa, S.; Tsuru, K. & Osaka, A. (2003). Apatite deposition on thermally and anodically oxidized titanium surfaces in a simulated body fluid. *Biomaterials*, 24, 4631-4631

Wang, Y.B. & Zheng, Y.F. (2009). Corrosion behaviour and biocompatibility evalution of low modulus Ti-16Nb shape memory alloy as potential biomaterial. *Material Letters*, 63, 1293-1295

Wang, J. T.; Weng, C. & Chang, J.G. (2000). The influence of temperature and surface conditions on surface absorptivity in laser surface treatment. *J Appl physics*, 87, 3245-3253

Wieland, M.; Textor, M.; Spencer, N.D. & Brunette, D.M. (2001). Wavelength-roughness: a quantitative approach to characterizing the topography of rough titanium surfaces. *Int JOral Maxilloface Impl*, 16(2), 163-181

Xiong, L. & Yang, L. (2003). Quantitative analysis of osteoblast behaviour on microgroovedhydroxyapatite and titanium substrata. *J Biomed. Mater. Res.*, 66A, 677-687

Yap, A.S. & Kovacs, E.M. (2003). Direct cadherin – activated cell signaling: a view from the plasma membrane. *J Cell Biol.*, 160, 11-16

Yamada, K. (1991). Adhesive recognition sequences. *J Biol. Chem.*, 266, 12809-12812

Yang, Y.C. & Change, E. (2001). Influence of residual stress on bonding strength and fracture of plasma–sprayed hydroxyapatite coatings on Ti-6AL-4V substrate. *Biomaterials*, 22, 1827-1836

Yang, J.; Lian, J.; Dong, Q. & Guo, Z. (2004). Nano structured films formed on the AlSi 329 stainless steel by Nd:YAG pulsed laser irradiation. *Appl. Surf. Sci.*, 229, 2-8

Ziats, N.P.; Miller, K.M. & Anderson, J.M. (1988). In vitro and in vivo interactions of cells with biomaterials. *Biomaterials, (Ibid)*, 9, 5-13

Zhu, X. & Assoian, R. K. (1995). Integrin-dependent activation of MAP kinase: a link to shape-dependent cell proliferation. *Mol. Biol. Cell*, 6, 273-282

Biomedical Engineering, Trends in Materials Science

Edited by Mr Anthony Laskovski

ISBN 978-953-307-513-6

Hard cover, 564 pages

Publisher InTech

Published online 08, January, 2011

Published in print edition January, 2011

Rapid technological developments in the last century have brought the field of biomedical engineering into a totally new realm. Breakthroughs in materials science, imaging, electronics and, more recently, the information age have improved our understanding of the human body. As a result, the field of biomedical engineering is thriving, with innovations that aim to improve the quality and reduce the cost of medical care. This book is the second in a series of three that will present recent trends in biomedical engineering, with a particular focus on materials science in biomedical engineering, including developments in alloys, nanomaterials and polymer technologies.

INTECH
open science | open minds